

Search for production of a single vectorlike quark decaying to tH or tZ in the all-hadronic final state in pp collisions at $\sqrt{s} = 13$ TeV

A. Hayrapetyan *et al.**
(CMS Collaboration)

 (Received 8 May 2024; accepted 13 September 2024; published 21 October 2024)

A search for electroweak production of a single vectorlike T quark in association with a bottom (b) quark in the all-hadronic decay channel is presented. This search uses proton-proton collision data at $\sqrt{s} = 13$ TeV collected by the CMS experiment at the CERN LHC during 2016–2018, corresponding to an integrated luminosity of 138 fb^{-1} . The T quark is assumed to have charge $2/3$ and decay to a top (t) quark and a Higgs (H) or Z boson. Hadronic decays of the t quark and the H or Z boson are reconstructed from the kinematic properties of jets, including those containing b hadrons. No deviation from the standard model prediction is observed in the reconstructed tH and tZ invariant mass distributions. The 95% confidence level upper limits on the product of the production cross section and branching fraction of a T quark produced in association with a b quark and decaying via tH or tZ range from 1260 to 68 fb for T quark masses of 600–1200 GeV.

DOI: [10.1103/PhysRevD.110.072012](https://doi.org/10.1103/PhysRevD.110.072012)

I. INTRODUCTION

Vectorlike quarks (VLQs) appear in many extensions of the standard model (SM) as they provide a solution to the hierarchy problem by protecting the Higgs (H) boson mass from large radiative corrections [1–4]. They are assumed to mix with the third-generation SM quarks, and in contrast to SM chiral quarks, have both vector and axial vectorlike couplings. These nonchiral couplings allow VLQs to avoid the strong experimental constraints, which now exclude additional generations of chiral quarks [5–7].

The VLQs can either be produced in pairs via the strong interaction or singly via the electroweak interactions, in association with additional quarks. Figure 1 shows a possible electroweak production diagram for a vectorlike top quark partner T of charge $2/3$. While the pair production cross section depends only on the T quark mass, the electroweak production of a single T quark depends on the initial-state coupling. These couplings are typically constrained to small values by precision measurements [2], thus resulting in low production cross sections. However, in some models, such as a composite Higgs scenario [8], a cross section of up to two orders of magnitude larger is possible.

The T quark may decay into a bottom (b) quark and a W boson (bW), a top (t) quark and a Z boson (tZ), or a top

quark and a Higgs boson (tH). The branching fractions are model dependent. For the singlet model presented in Ref. [9], the branching fractions are 50% for decays to bW and 25% each for decays to tZ or tH . In contrast, if the T quark occurs in a doublet with a vectorlike bottom quark partner B of charge $-1/3$, its branching fractions is 50% for decays to either tZ or tH .

We search for electroweak production of a T quark in association with a b quark, which requires a nonzero TWb coupling for production. We consider a T quark with a narrow width ($\Gamma/M \lesssim 1\%$) in the singlet model with a 50% branching fraction to bW and 25% branching fractions each to tZ and tH .

The ATLAS and CMS Collaborations have reported many searches for pair production of narrow-width VLQs in various final states using proton-proton (pp) collisions at $\sqrt{s} = 13$ TeV [10–14]. Both Collaborations have set constraints on electroweak production of VLQs [15–17]. The CMS Collaboration has searched for $T \rightarrow bW$ [18], tZ [19,20], and tH [21,22], primarily focusing on signatures with a large Lorentz boost of the T quark decay products.

In the fully hadronic final state, a signature of single T quark production is a resonant peak in the reconstructed $t + b\bar{b}$ mass distribution, with the $b\bar{b}$ pair originating from the decay of either a H or Z boson. Events with five jets consistent with hadronic decays of a top quark and a H or Z boson are selected. The reconstruction of the H or Z boson candidate is achieved using b tagging techniques and dedicated kinematic selections. This signature is particularly effective for T masses when the final state jets can be resolved. For masses above 1000 GeV, some decay products may merge into a single jet, requiring targeted

*Full author list given at the end of the article.

Published by the American Physical Society under the terms of the [Creative Commons Attribution 4.0 International license](https://creativecommons.org/licenses/by/4.0/). Further distribution of this work must maintain attribution to the author(s) and the published article's title, journal citation, and DOI. Funded by SCOAP³.

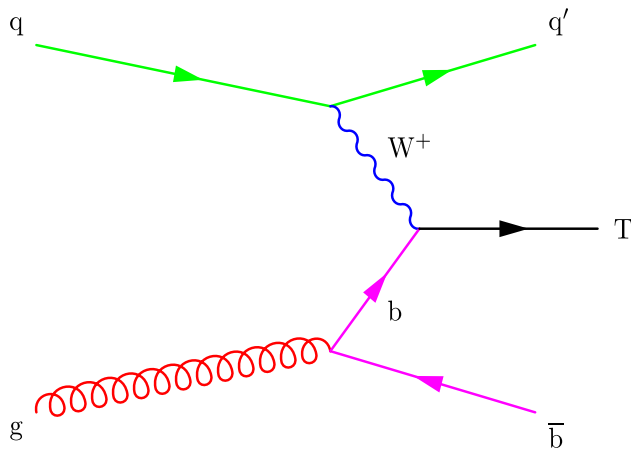


FIG. 1. Example of Feynman diagram for electroweak production of a vectorlike T quark.

reconstruction algorithms not considered in this analysis. The search presented in this paper uses pp collision data collected at $\sqrt{s} = 13$ TeV over the 2016, 2017, and 2018, and corresponds to an integrated luminosity of 138 fb^{-1} . The analysis is focused on T quark masses between 600–1200 GeV and extends results reported by CMS in Ref. [23] that are based on the 2016 data.

The paper is organized as follows. In Sec. II the CMS detector and event reconstruction are described, modeling of signal and background processes is discussed in Sec. III. Methods for reconstructing the T quark mass and event selection are presented in Sec. IV, and background estimation method is described in Sec. V. Section VI discusses the systematic uncertainties considered, results are shown in Sec. VII and a summary is given in Sec. VIII.

II. THE CMS DETECTOR AND EVENT RECONSTRUCTION

The central feature of the CMS apparatus is a superconducting solenoid of 6 m internal diameter, providing a magnetic field of 3.8 T. Within the solenoid volume are a silicon pixel and strip tracker, a lead tungstate crystal electromagnetic calorimeter (ECAL), and a brass and scintillator hadron calorimeter (HCAL), each composed of a barrel and two endcap sections. Forward calorimeters extend the pseudorapidity (η) coverage provided by the barrel and endcap detectors. Muons are detected in gas-ionization chambers embedded in the steel flux-return yoke outside the solenoid.

The silicon tracker used in 2016 measured charged particles within the range $|\eta| < 2.5$. For nonisolated particles of transverse momentum $1 < p_T < 10$ GeV and $|\eta| < 1.4$, the track resolutions were typically 1.5% in p_T and 25–90 (45–150) μm in the transverse (longitudinal) impact parameter [24]. At the start of 2017, a new pixel detector was installed [25]; the upgraded tracker measured particles up to $|\eta| < 3.0$ with typical resolutions of 1.5% in

p_T and 20–75 μm in the transverse impact parameter [26] for nonisolated particles of $1 < p_T < 10$ GeV.

The electron momentum is estimated by combining the energy measurement in the ECAL with the momentum measurement in the tracker. The momentum resolution for electrons with $p_T \approx 45$ GeV from $Z \rightarrow ee$ decays ranges from 1.6 to 5%. It is generally better in the barrel region than in the end caps, and also depends on the bremsstrahlung energy emitted by the electron as it traverses the material in front of the ECAL [27,28]. In the region $|\eta| < 1.74$, the HCAL cells have widths of 0.087 in pseudorapidity and 0.087 in azimuth (ϕ). In the $\eta - \phi$ plane and for $|\eta| < 1.48$, the HCAL cells map on to 5×5 arrays of ECAL crystals to form calorimeter towers projecting radially outwards from close to the nominal interaction point. For $|\eta| > 1.74$, the coverage of the towers increases progressively to a maximum of 0.174 in $\Delta\eta$ and $\Delta\phi$. Within each tower, the energy deposits in ECAL and HCAL cells are summed to define the calorimeter tower energies, subsequently used to provide the energies and directions of hadronic jets.

A more detailed description of the CMS detector, together with a definition of the coordinate system used and the relevant kinematic variables, can be found in Ref. [29].

Events of interest are selected using a two-tiered trigger system [30]. The first level, composed of custom hardware processors, uses information from the calorimeters and muon detectors to select events at a rate of around 100 kHz within a fixed time interval of about 4 μs . The second level, known as the high-level trigger, consists of a farm of processors running a version of the full event reconstruction software optimized for fast processing, and reduces the event rate to around 1 kHz before data storage.

The primary pp interaction vertex is taken to be the vertex corresponding to the hardest scattering in the event, evaluated using tracking information alone, as described in Sec. 9.4.1 of Ref. [31].

The particle-flow (PF) algorithm [32] aims to reconstruct and identify each individual particle (PF candidate) in an event, with an optimized combination of information from the various elements of the CMS detector. The energy of photons is obtained from the ECAL measurement. The energy of electrons is determined from a combination of the electron momentum at the primary interaction vertex as determined by the tracker, the energy of the corresponding ECAL cluster, and the energy sum of all bremsstrahlung photons spatially compatible with originating from the electron track. The energy of muons is obtained from the curvature of the corresponding track. The energy of charged hadrons is determined from a combination of their momentum measured in the tracker and the matching ECAL and HCAL energy deposits, corrected for the response function of the calorimeters to hadronic showers. Finally, the energy of neutral hadrons is obtained from the corresponding corrected ECAL and HCAL energies.

The current search targets hadronic decays of the vector-like T quark that result in at least five jets in the final state. Jets are reconstructed offline from the energy deposits in the calorimeter towers, clustered using the anti- k_T algorithm [33,34] with a distance parameter of 0.4. In this process, the contribution from each calorimeter tower is assigned a momentum, the absolute value and the direction of which are given by the energy measured in the tower, and the coordinates of the tower. The raw jet energy is obtained from the sum of the tower energies, and the raw jet momentum by the vectorial sum of the tower momenta, which results in a nonzero jet mass. The raw jet energies are then corrected to establish a uniform relative response of the calorimeter in η and a calibrated absolute response in p_T . Additional pp interactions within the same or nearby bunch crossings (pileup) can contribute additional tracks and calorimetric energy depositions, increasing the apparent jet momentum. To mitigate this effect, tracks identified to be originating from pileup vertices are discarded, and an offset correction is applied to correct for remaining contributions [35]. Jet energy corrections are derived from simulation studies so that the average measured energy of jets becomes identical to that of particle-level jets. In situ measurements of the momentum balance in dijet, photon + jet, Z + jet, and multijet events are used to determine any residual differences between the jet energy scale in data and in simulation, and appropriate corrections are made [36]. Additional selection criteria are applied to each jet to remove jets potentially dominated by instrumental effects or reconstruction failures [35]. The jet energy resolution amounts typically to 15–20% at 30 GeV, 10% at 100 GeV, and 5% at 1 TeV [36].

Jets originating from the hadronization of a bottom quark can be tagged as b jets. The DeepCSV discriminator is used [37]. It relies on a deep neural network trained to classify the different jet flavors using information from the tracks and secondary vertices. Three working points [37] are defined: loose, medium, and tight, which correspond to a misidentification rate for light quark or gluon jets of 10, 1, and 0.1%, respectively. The efficiency for these working points, as measured in simulated samples of top quark-antiquark ($t\bar{t}$) production, ranges from around 80% for the loose working point to around 45% for the tight one.

III. MODELING OF SIGNALS AND BACKGROUNDS

Simulated samples for the signal process, $pp \rightarrow Tbq$ with the T quark decaying to a t quark and either a Higgs or a Z boson, are generated at leading order (LO) using the Monte Carlo (MC) event generator MadGraph5_aMC@NLO [38] 2.2.2 (for data recorded in 2016) and 2.4.2 (for data recorded in 2017–2018). The T quark is assumed to have a width of 10 GeV, which is small compared to the experimental resolution, and left-handed chirality. The mass of the top quark is set to 172.5 GeV and the mass

of the Higgs boson to 125 GeV. Both particles decay inclusively, with $\mathcal{B}(H \rightarrow b\bar{b})$ set to 58% [39].

The MadGraph5_aMC@NLO generator is interfaced with PYTHIA 8.212 [40] for the description of parton fragmentation and hadronization, using CUETP8M1 [41] (2016) and CP5 [42] (2017 and 2018) underlying event tunes. Parton distribution function (PDF) sets used are LO NNPDF 3.0 [43] (2016) and next-to-next-to-LO NNPDF 3.1 [44] (2017 and 2018). Simulation of the CMS detector is based on Geant4 [45]. Simulated minimum-bias events are mixed with the hard interactions in simulated events to reproduce the effect of pileup. Finally, all simulated events are reweighted such that the distribution of the number of collisions per bunch crossing matches the one observed in data, with an average of approximately 23 (32) [46–48] in 2016 (2017–2018).

The $t\bar{t}$ events that are simulated with POWHEG 2.0 [49–52] are used to cross check details of the analysis. The same generator is used for the single top quark production. Simulated events from other SM background processes are used for cross checking the analysis strategy. The MadGraph5_aMC@NLO generator is used to simulate the SM Higgs boson production in association with top quarks (tH , $t\bar{t}H$) [53], or with a vector boson (VH) [54]. The background processes W/Z + jets are simulated with MadGraph5_aMC@NLO. Diboson and other SM events composed uniquely of jets produced through the strong interaction, referred to as quantum chromodynamics (QCD) multijet events, are produced at the leading order with PYTHIA 8.205 [40]. The PDF sets are identical to the signal ones and both change with the year.

The analysis uses data directly to estimate the background.

IV. EVENT SELECTION

The analysis targets the decay of a T quark to a top quark and a Higgs or Z boson, where $t \rightarrow bW \rightarrow bqq'$ and $H/Z \rightarrow b\bar{b}$. The final state is composed of at least seven jets, where five of them arise from the T quark decay, three of which are b jets. As shown in Fig. 1, when the T quark is singly produced, two additional jets are present in the event.

Events are selected online using a combination (logical “OR”) of hadronic trigger criteria. These triggers require a scalar p_T sum of the jets (H_T) above a certain threshold: 400 GeV in 2016, and 300 GeV in 2017 and 2018. For the 2016 data, this combination includes a trigger requiring at least six jets with $p_T > 30$ GeV, with at least two of them passing the online b tagging criteria. For the 2017 and 2018 data-taking years, two main trigger paths are used: one requiring at least four jets with three of them b tagged, and a second requiring at least six jets with two of them b tagged. For these triggers, the jet p_T threshold was increased to 32 GeV. The trigger efficiency with respect to the offline selection is measured in data and found to be about 97% for 2016, 95% for 2017, and 97% for 2018 with

a dedicated trigger path. The set of triggers records events with an invariant mass of around 300 GeV or above.

The invariant mass reconstructed from five jets is used as the main discriminating variable. In the fully hadronic final state, the main background processes are multijet and $t\bar{t}$ + jets events. Signal events are expected to exhibit a peak in the five-jet invariant mass distribution at the resonance mass, while background events, in the absence of selection criteria, would have a smoothly falling shape.

Based on the online requirements, at least six jets with $p_T > 40$ GeV and $|\eta| < 4.5$ are required offline. As signal jets result from the decay of a high-mass resonance, the p_T thresholds are increased to 170, 130, and 80 GeV for the leading, second-leading, and third-leading jets, respectively. In addition, at least three b -tagged jets using the tight DeepCSV working point [37] are required among the jets with $|\eta| < 2.4$ (2.5) in 2016 (2017 and 2018) data. The $|\eta|$ range is extended in 2017 and 2018 data because of the increased coverage of the upgraded pixel detector [25].

A. Identification of T quark candidates

A multistep χ^2 minimization algorithm is used to identify the best Higgs or Z boson and top quark candidates among all five-jet combinations as in Ref. [23]. Resonance mass peaks are expected for the $H/Z/W$ boson and the top quark, which are examined to increase the efficiency of identifying the correct jet assignment.

The algorithm first minimizes $\chi_{H/Z}^2$, defined as

$$\chi_{H/Z}^2 = \left(\frac{m_{H/Z}^{\text{meas}} - \mu_{H/Z}^{\text{MC}}}{\sigma_{H/Z}^{\text{MC}}} \right)^2, \quad (1)$$

where $m_{H/Z}^{\text{meas}}$ is the measured invariant mass of a given pair of b -tagged jets and $\mu_{H/Z}^{\text{MC}}$ and $\sigma_{H/Z}^{\text{MC}}$ denote the expected mean and standard deviation mass values obtained from Gaussian fits to the distribution of the invariant mass computed from matched reconstructed jets in simulated signal samples. The reconstructed jets are matched to the generated particles if the ΔR between them is less than 0.4. The minimization is performed over all possible pairs of b -tagged jets. The chosen b -tagged jets are removed from consideration for the subsequent steps.

The remaining jets are considered for forming a W boson candidate, consisting of two jets, and a top quark candidate, consisting of the W boson candidate and an additional b -tagged jet. For these candidates, χ_W^2 and χ_t^2 are calculated as

$$\begin{aligned} \chi_W^2 &= \left(\frac{m_W^{\text{meas}} - \mu_W^{\text{MC}}}{\sigma_W^{\text{MC}}} \right)^2, \\ \chi_t^2 &= \left(\frac{m_t^{\text{meas}} - \mu_t^{\text{MC}}}{\sigma_t^{\text{MC}}} \right)^2, \end{aligned} \quad (2)$$

with the analogous definitions of m^{meas} , μ^{MC} , and σ^{MC} for each resonance. Finally, the total χ^2 function

TABLE I. Mean and standard deviation values from a Gaussian fit of the $H/Z/W$ boson and top quark mass distributions in the 700 GeV T quark sample, requiring the jet kinematic criteria described above and matching to generated particles. All quantities are in units of GeV. The year-to-year variations are within the jet energy scale uncertainties.

Particle	2016		2017		2018	
	μ^{MC}	σ^{MC}	μ^{MC}	σ^{MC}	μ^{MC}	σ^{MC}
H	121.9	13.5	118.9	14.7	120.2	14.3
Z	90.9	11.4	89.2	12.0	90.9	11.3
W	83.8	10.9	82.5	12.6	83.9	10.8
t	173.8	16.0	172.8	18.9	175.9	17.2

$$\chi^2 = \chi_{H/Z}^2 + \chi_W^2 + \chi_t^2 \quad (3)$$

is minimized using all possible jet combinations for the W boson and top quark candidates. This multistep procedure improves the signal-to-background ratio for a signal with a T mass of 700 GeV by 30% compared to simply choosing the jet combination with the best total χ^2 .

The values used for the particle mass mean and standard deviation are given in Table I and vary slightly for each data-taking year. Using masses obtained by fitting the signal MC samples, improves the signal efficiency by 1–3% compared to using world-average values.

B. Mass categorization

We impose additional selection criteria to reduce the background contribution and ensure correct identification of the $H/Z/W$ boson and top quark candidates. In addition to the kinematic selection described above, the baseline selection includes the following criteria.

- (i) The total $\chi^2 < 15$.
- (ii) The reconstructed Higgs (Z) boson must have a mass larger (smaller) than 100 GeV. This ensures the two channels do not overlap.
- (iii) The “second top quark mass” is defined as the invariant mass of the H/Z candidate and the highest p_T jet that is not used to form the primary top quark candidate. The second top quark mass must be greater than 250 GeV.

The second top quark mass requirement removes a large fraction of $t\bar{t}$ events while retaining nearly all signal events, improving the signal-to- $t\bar{t}$ ratio by more than 10%. Although three b -tagged jets are required in the signal region (SR) of this search, a charm (c) quark from the W boson decay misidentified as a b quark could form a H/Z boson candidate with the genuine b quark from the other top quark decay. The c quark misidentification by the b tagging algorithms, which is at the level of a few percent, introduces a large $t\bar{t}$ background. These events are more likely than signal events to contain a second top quark candidate with a mass near 172 GeV.

Further selection criteria, described below, are intended to improve the quality of the $H/Z/W$ boson, and top quark candidates to reduce the background. These criteria are chosen to be as model-independent as possible.

Different selection criteria are used for low- and high-mass T quark candidates in the mass range 600–800 and above 800 GeV, respectively. The variables used for both selections are the same and are identical to those used in an earlier version of the analysis [23]. The high-mass selection consists of simple fixed-threshold requirements on the variables, while the low-mass requirements are chosen to avoid distorting the five-jet invariant mass distribution and producing artificial peaks.

The SR with the highest signal-to-background ratio is the 3T one requiring three tight b -tagged jets. The 3M SR contains events with three medium b -tagged jets, but no events with three tight b -tagged jets. The 2M1L SR contains events with two medium and one loose b -tagged jets, but no events with three medium b -tagged jets. These conditions, along with the 3T SR, create three mutually exclusive regions. The 2M1L SR is enriched in background events, while the 3M region provides a transition region between background- and signal-enriched regions. Both regions have kinematic distributions similar to the 3T region.

1. High-mass T selection

High efficiency for T quark masses above 800 GeV is achieved through selection criteria that are independent of the reconstructed T quark mass.

- (i) We require relative H_T , defined as the scalar p_T sum of the H/Z boson and t quark candidates divided by the total H_T of the event (scalar p_T sum of all jets with $p_T > 30$ GeV in the event) to be greater than 0.4. In single T quark production most of the momentum is carried by the top quark and H/Z boson, therefore the relative H_T discriminates against $t\bar{t}$ and QCD multijet events.

- (ii) We require $\max(\chi_{H/Z}^2, \chi_W^2, \chi_t^2) < 3.0$. The individual χ^2 values are required to have small values to decrease the rate of $H/Z/W/t$ misidentification. This criterion effectively imposes a mass window of no more than $\pm\sqrt{3}$ times the mass resolution for each candidate.
- (iii) $\Delta R < 1.1$ separation is required between $b_{H/Z}$ and $\bar{b}_{H/Z}$ jets that form the H/Z candidate where $\Delta R = \sqrt{(\Delta\eta)^2 + (\Delta\phi)^2}$ and $\Delta\eta$ and $\Delta\phi$ are the separations in pseudorapidity and azimuthal angle, respectively. In signal events, the H/Z boson tends to have a moderate Lorentz boost ($p_T \lesssim 400$ GeV), such that the two b -tagged jets are near each other without being completely merged.
- (iv) For the tH (tZ) channel, we require $\chi_{H/Z}^2 < 1.5$ (1.0) because almost all background events do not contain a genuine H/Z boson. This criterion is equivalent to a mass window of ± 17 (12) GeV around the H (Z) boson mass.
- (v) We require $\Delta R(j_W, j'_W) < 1.75$ between two jets j_W, j'_W comprising the W boson candidate because most signal events contain W bosons with moderate Lorentz boost.
- (vi) We also require $\Delta R(b_t, W) < 1.2$ between the b jet forming the top quark candidate and the W boson candidate because most signal events contain top quarks with moderate Lorentz boost.

The Table II summarizes the selection criteria for the signal regions. In the SR, called the 3T region, we additionally require three jets passing the tight b tagging criterion of the DeepCSV algorithm, yielding 1256 events in data with 15.1 signal events expected for a T quark mass of 900 GeV. The estimated selection efficiencies for a 900 GeV T quark signal and various background processes in the tH channel and the 2016 data-taking year are presented in Table III. The efficiencies vary slightly in the 2017 and 2018 data-taking years.

TABLE II. Definitions of the signal and control regions for the high-mass selection. If the same selection is applied in all SRs and CRs, this is indicated by the \div symbol in the latter. If no selection is applied, this is indicated by the ... symbol. The “3T,” “3M,” and “2T1L/2M1L” represent region with three tight, three medium, and two tight/medium plus one loose b tagging requirements on the jets, respectively.

Requirement	SR 3T/3M/2M1L	CR Multijet 3T/3M/2M1L	CR $t\bar{t}$ 2T1L/2M1L
t quark candidate b -tagged jet	T/M
χ^2	<15	<50	<50
Relative H_T	>0.4	\div	\div
$\max(\chi_{H/Z}^2, \chi_W^2, \chi_t^2)$	<3	5–20	3–5
χ_t^2	<3	>1	<1.5
$\Delta R(b_{H/Z}, \bar{b}_{H/Z})$	<1.1	\div	<1.5
$\chi_{H/Z}^2$ (tH channel)	<1.5	\div	<3.0
$\chi_{H/Z}^2$ (tZ channel)	<1.0	\div	<3.0
$\Delta R(j_W, j'_W)$	<1.75	\div	\div
$\Delta R(b_t, W)$	<1.2	\div	\div

TABLE III. Cumulative efficiencies of the high-mass selection criteria for signal and various simulated backgrounds in 2016 data. The first and last lines indicate the expected number of events normalized to an integrated luminosity of 35.9 fb^{-1} . Only statistical uncertainties are reported. The “Other backgrounds” column includes $W/Z + \text{jets}$, single t , $t\bar{t}H$, and $t\bar{t}Z$ background processes. The $t\bar{t}H$ and $t\bar{t}Z$ processes do not form a resonance and have production rates roughly the same as the signal rate.

Cuts	T (900 GeV)	Multijet	$t\bar{t}$	Other backgrounds
Baseline selection (35.9 fb^{-1})	9.5 ± 0.3	9360 ± 810	2610 ± 30	353 ± 23
Relative H_T	89.5%	42.8%	51.9%	52.9%
$\max(\chi_{H/Z}^2, \chi_W^2, \chi_t^2)$	55.9%	14.1%	25.1%	21.8%
$\Delta R(b_{H/Z}, \bar{b}_{H/Z})$	51.1%	7.5%	11.9%	8.9%
$\chi_{H/Z}^2$	45.6%	4.9%	9.3%	7.1%
$\Delta R(j_W, j'_W)$	39.2%	3.2%	7.2%	5.6%
$\Delta R(b_t, W)$	34.1%	1.9%	4.5%	2.5%
High-mass selection (35.9 fb^{-1})	3.2 ± 0.2	181 ± 52	117 ± 6	9.3 ± 0.6

Such a selection has the drawback of sculpting the five-jet invariant mass distribution as shown in Fig. 2.

2. Low-mass T selection

For the low-mass T selection, we first identify the criteria listed above that modify the five-jet invariant mass distribution. The two χ^2 criteria do not affect the five-jet invariant mass distribution, therefore the corresponding selections are unchanged.

For the other selection criteria, the threshold values are modified depending on the five-jet invariant mass in order to preserve the shape of the five-jet invariant mass falling

spectrum. We consider the distributions of the variables $\Delta R(b_{H/Z}, \bar{b}_{H/Z})$, $\Delta R(j_W, j'_W)$, relative H_T , and $\Delta R(b_t, W)$ in bins of the five-jet invariant mass. For each mass bin, a threshold is defined in order to keep a given fraction of events. The resulting threshold values for a given variable are fit as a function of the five-jet invariant mass. These fitted functions represent the mass-dependent criteria for each variable. The quantile is chosen to provide the same signal efficiency as the high-mass selection for a T quark mass of 700 GeV.

The functions obtained from this procedure are polynomials of degree 5–7. To mitigate the potentially large systematic uncertainty from the limited size of the MC sample of events with at least 3 tight b -tagged jets, data are used directly. The functions are derived using events from 2018 data in the two medium and one loose b -tagged jet (2M1L) region, which excludes events with three medium b -tagged jets. To test for potential bias from the particular choice of function, we perform studies using alternative functional forms. The presence of signal contamination at the signal strengths considered in this analysis would also have a negligible effect on the background model. We find that neither small signal contamination nor the particular choice of function biases the selection. The same functions are applied to the tH and tZ channels and to the other data-taking years. As the low-mass selection always preserves the same fraction of events regardless of the five-jet invariant mass, for larger masses, the number of events is reduced compared to the high-mass selection corresponding to a lower signal efficiency. Figure 2 compares the five-jet invariant mass distributions (M_{tH}) after the low- and high-mass selections in the 2M1L region of the tH channel in 2018 data. With the low-mass selection, the five-jet invariant mass distribution is a smoothly falling spectrum above 400 GeV.

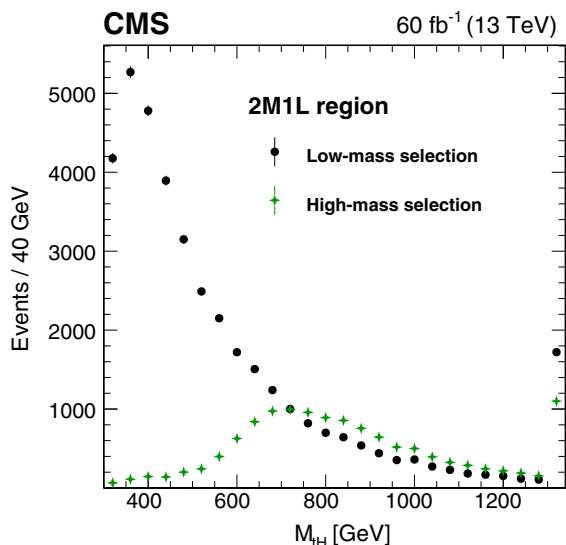


FIG. 2. The five-jet invariant mass distribution in the 2M1L region after the high-mass (green crosses) and low-mass (black circles) selections in 2018 data. The rightmost bin of the distribution is an overflow bin. The low-mass selection results in a mass distribution that is smoothly falling, unlike the high-mass selection. The high-mass selection is more efficient for T quark masses above 700 GeV by up to 25% while maintaining a similar background level, as detailed in Sec. IV B 1.

V. BACKGROUND ESTIMATION AND VALIDATION

While signal events follow a resonance in the five-jet invariant mass, SM background events, without any

selection, form a smoothly falling distribution. The background distribution is inferred from regions with relaxed b tagging requirements. As described in Sec. IV B, the high-mass selection sculpts the mass distribution. The validation of the background estimation method is mainly conducted in this region as it has a more complex shape.

As the selection variables are not correlated with the b tagging criteria, the shape of the five-jet invariant mass distribution for the SM backgrounds can be modeled from data in regions with loosely b -tagged jets without introducing a significant bias.

The background-dominated regions are defined by relaxing the b tagging requirements on three jets used to form the T quark candidate. With the large sample sizes in the 2M1L SR, the background distributions are determined with high statistical precision.

The background prediction is constructed bin by bin using a simultaneous binned maximum likelihood fit. For each bin of the five-jet invariant mass, the total expected

Poisson mean yield under the signal-plus-background hypothesis is composed of a background component and a signal component scaled by the signal strength μ ,

$$\begin{aligned}\lambda_{3T} &= \lambda_{3T}^B + \mu\lambda_{3T}^S \\ \lambda_{3M} &= \lambda_{3M}^B + \mu\lambda_{3M}^S \\ \lambda_{2M1L} &= \lambda_{2M1L}^B + \mu\lambda_{2M1L}^S,\end{aligned}\quad (4)$$

where λ_X , λ_X^B , and λ_X^S represent the expected total, background, and signal yields in a given bin and region X, respectively. Each λ_X^S is determined from simulation. The transfer functions connect the predictions in different regions,

$$\begin{aligned}\lambda_{3T}^B &= N_{3M \rightarrow 3T} f_{3M \rightarrow 3T} \lambda_{3M}^B \\ \lambda_{3M}^B &= N_{2M1L \rightarrow 3M} f_{2M1L \rightarrow 3M} \lambda_{2M1L}^B,\end{aligned}\quad (5)$$

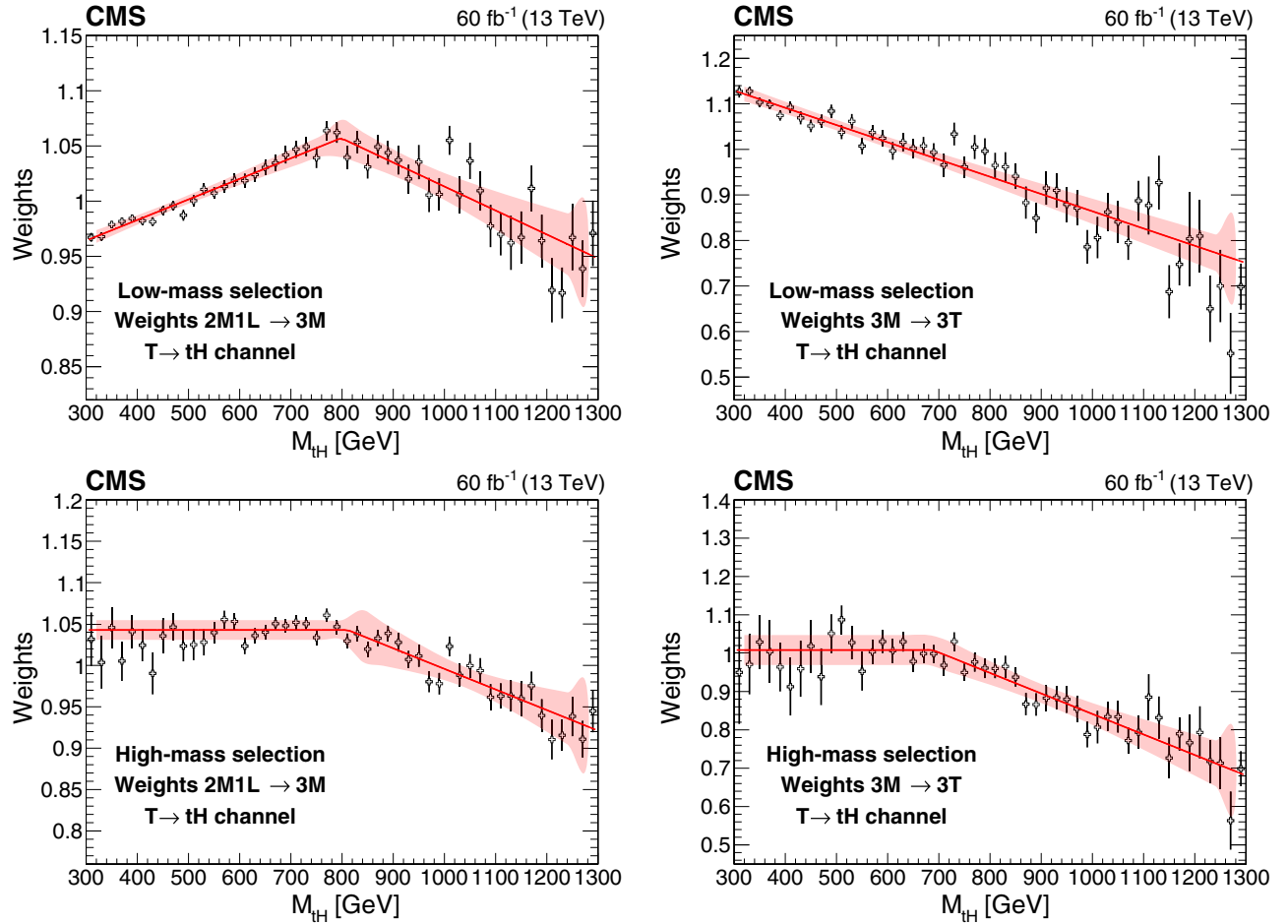


FIG. 3. Weights from b tagging ratios (open markers) as functions of the five-jet invariant mass in 2018 data for the low-mass (upper) and high-mass (lower) selections. The left graphs show weights connecting the 2M1L and 3M regions, and the right graphs show weights connecting the 3M and 3T regions. The red line corresponds to the central value of the transfer function and the shaded area represents the 95% confidence level uncertainty band. For the low-mass (high-mass) analysis only signals with mass below (above) 800 GeV are tested, so primarily the lower (upper) part of the distribution contributes to the final result.

where $N_{X \rightarrow Y}$ is an overall normalization factor, which corresponds to the ratio of the overall selection efficiency for region Y to that for region X and $f_{X \rightarrow Y}$ is the value of the transfer function from region X to Y for a given bin correcting for small efficiency differences between the regions as described below. The two normalization factors, signal strength, and $\lambda_{2\text{MIL}}^B$ are simultaneously determined during the fit to data. The fit procedure incorporates the systematic uncertainties as nuisance parameters described in the next section.

The transfer function accounts for b tagging efficiencies for a given b tagging working point to vary slightly depending on the b -tagged jet kinematics. To correctly model the background shape in a region with different b tagging criteria, we reweight events based on the ratio of jets between loose and medium b -tagged jets, and between medium and tight b -tagged jets obtained in the multijet validation sample described below after requiring the baseline criteria. Since p_T and η are highly correlated, we parametrize the ratios as functions of the total jet momentum and η .

The weight applied to each jet is calculated according to its kinematics, and the total event weight is the product of all the jet weights. This event weight corrects for the difference in kinematics in b tagging efficiency between the 3M and 3T (or 2T1L, corresponding to two tight and one loose b -tagged jets) regions, and between the 2M1L and 3M regions.

Transfer functions are derived by fitting a combination of two linear functions continuous at their connection to the weight distributions as functions of the five-jet invariant mass. One transfer function connects the 3M and 3T regions, and a second transfer function connects the 2M1L and 3M regions. Figure 3 shows both transfer functions for the low- and high-mass selections in the tH channel for the 2018 data. The difference between the functions for the two selections is largely driven by the difference in the five-jet invariant mass shapes. Similar functions are observed for the tZ channel and the other data-taking years. The range of the corrections is up to 5% for the transfer function from the 2M1L to the 3M SRs and up to 30% for the high-mass transfer function from 3M SR to the 3T SR.

The background shape estimation method is validated in control regions (CRs) enriched in multijet or $t\bar{t}$ events where similar subsamples with different b tagging criteria are defined. Both samples include events with total $\chi^2 < 50$. The multijet sample requires the maximum individual particle χ^2 to be in the range 5–20, while the $t\bar{t}$ sample requires it to be in the range 3–5. Both validation samples are mutually exclusive from the SRs where the maximum individual particle χ^2 is less than 3. In addition, the QCD multijet sample requires $\chi_t^2 > 1$ to reduce the number of $t\bar{t}$ events, while the $t\bar{t}$ sample requires $\chi_t^2 < 1.5$ along with an inverted $\chi_{H/Z}^2 > 1.5$ (1.0) requirement for the tH (tZ) channel. The QCD multijet sample consists of approximately 80% QCD multijet events and 20% $t\bar{t}$ events

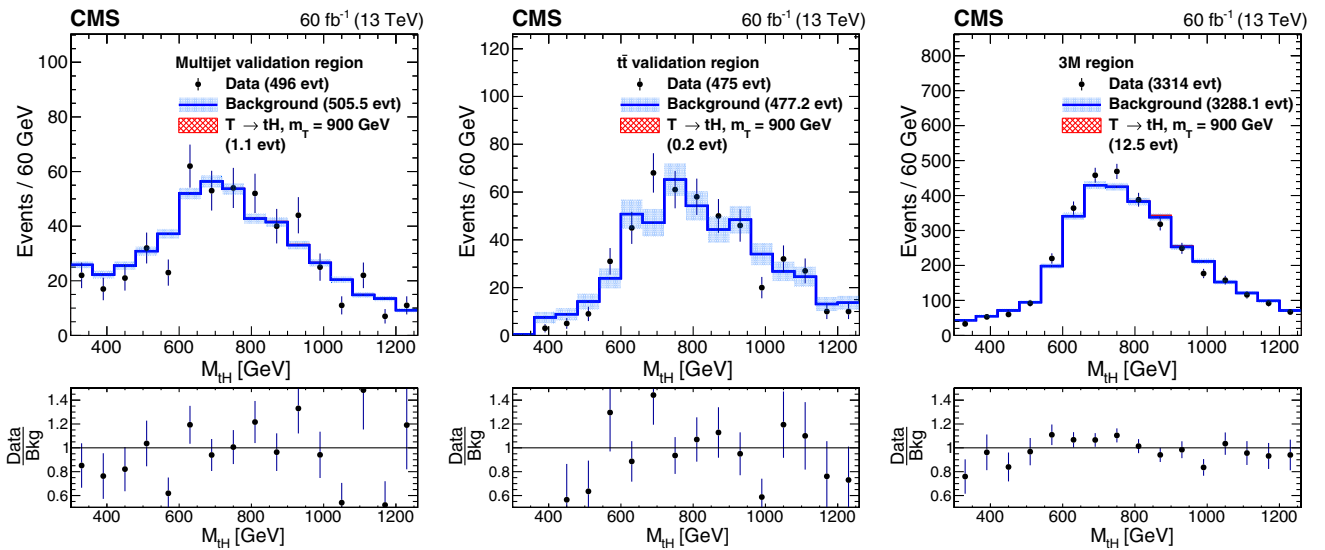


FIG. 4. The five-jet invariant mass distribution in the tH channel (black markers) after the high-mass selection in the QCD multijet 3T control region (left), the $t\bar{t}$ 2T1L control region (middle), and the 3M signal region (right) for the 2018 data. The histograms are the corresponding reweighted 2M1L distributions. The background distribution is normalized to the number of entries in the data. The shaded area corresponds to the statistical uncertainties in the 2M1L control regions. A potential 900 GeV T signal (red cross-hatched histogram) is added to the background histogram demonstrating a negligible contribution. Similar results are observed in the tZ channel, and for the other years, but with slightly larger statistical uncertainties.

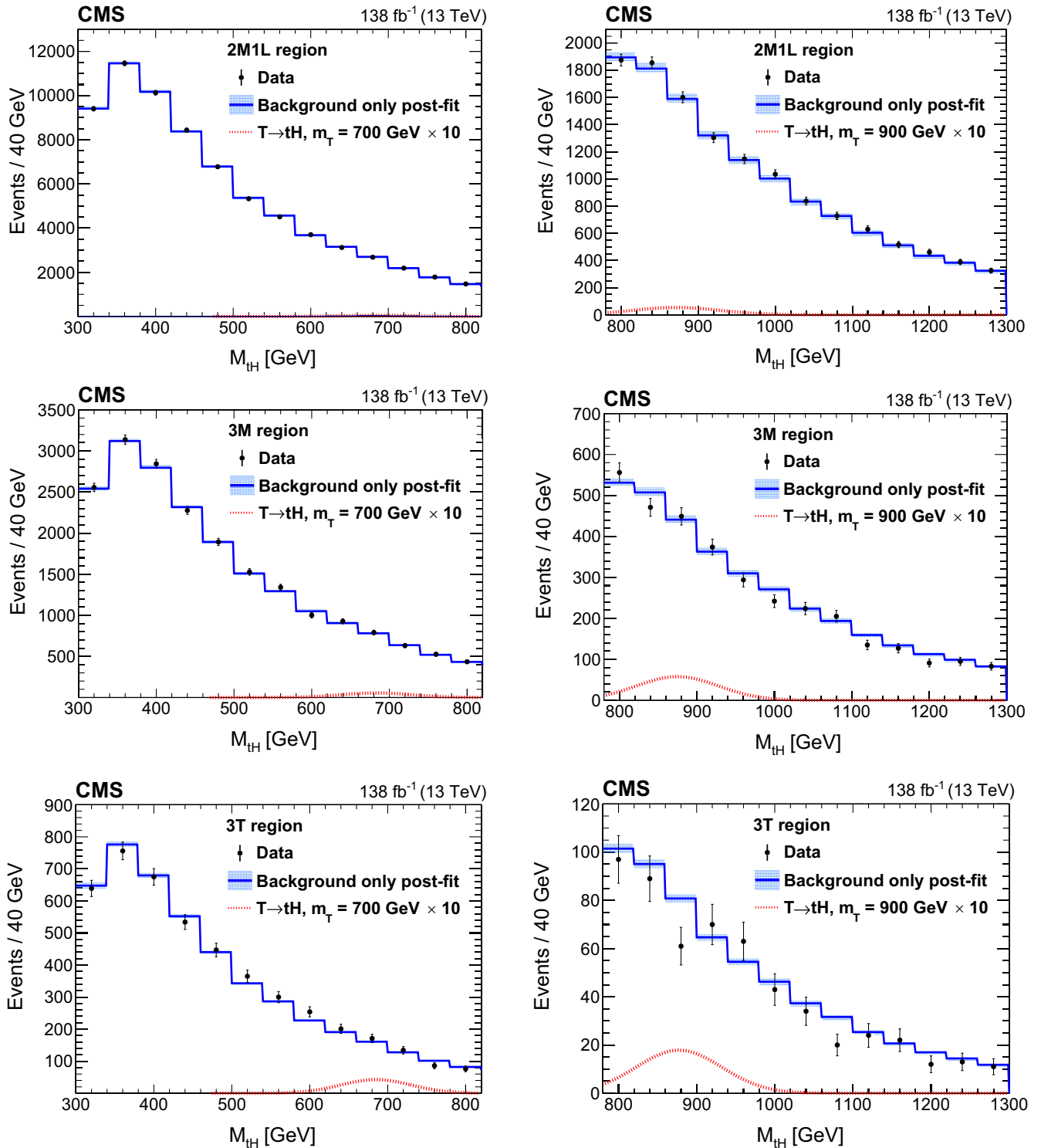


FIG. 5. Five-jet invariant mass distributions after a background-only fit (blue histogram) to the complete dataset (black markers) in the 2M1L (upper), 3M (middle), and 3T (lower) regions for low-mass (left) and the high-mass (right) selections. The dashed blue band represents the uncertainty on the fitted background estimate, and red dashed line shows the expected signal distribution for a 700 GeV (low-mass selection) and a 900 GeV (high-mass selection) T quark. The fit is performed on the combined data from all three years in the all- tH channel.

while the $t\bar{t}$ sample contains approximately 70% $t\bar{t}$ events and 30% QCD multijet events. Both samples are further subdivided by the b tag content using the same criteria as the background-dominated SRs described previously.

The $t\bar{t}$ sample is split into two mutually exclusive 2M1L and 2T1L regions. In the 2T1L (2M1L) $t\bar{t}$ CR, one of the tight (medium) b -tagged jets must form part of the t quark candidate. Table II summarizes the definition of the signal

region and control regions for the high-mass selection, highlighting the differences required to separate the samples. In addition to these two CRs for the tH and tZ channels, more CRs are created by changing the μ_i^{MC} input to the χ^2 variable: instead of setting it to the top quark mass, the value is fixed to either 140 or 250 GeV. Regions analogous to those in Table II are then defined leading to five additional CRs. The CRs with $\mu_i^{\text{MC}} = 250$ GeV contain fewer events than the others. The fraction of expected signal events is $\approx 3\%$ in the QCD multijet CR and $\approx 1\%$ in the $t\bar{t}$ CR.

Validation of the background model is performed in the QCD multijet and $t\bar{t}$ CRs. Events in the 2M1L CRs are reweighted to model the five-jet invariant mass distributions in the QCD multijet 3T or 3M CRs or $t\bar{t}$ 2T1L CRs. Kolmogorov-Smirnov tests [55–57] are used to compare the reweighted distributions with the data in the tighter regions, and they are found to be consistent with each other. Figure 4 shows the five-jet invariant mass distributions in the CRs (QCD multijet 3T and $t\bar{t}$ 2T1L) and the 3M SR in 2018 data, with the prediction from the corresponding reweighted 2M1L distributions. A potential signal with a mass of 900 GeV is overlaid. The shapes are similar in 2016 and 2017 data, and in the tZ channel. In total, 45 CRs have been examined.

VI. SYSTEMATIC UNCERTAINTIES

The systematic uncertainties in the analysis can be divided into two categories: those that affect the overall yields of the signal and background processes and those that affect the shape of the invariant mass distributions. A 3 (5)% uncertainty, uncorrelated between years, is assigned to the trigger efficiency for the 2016 (2017 and 2018) data. The jet energy scale and resolution uncertainties affect the overall normalization and shapes of the signal mass distributions, leading to changes of a couple of percent in the mean and sigma of the Gaussian. Correlations among the years are taken into account. The b tagging efficiency scale factor uncertainties for jets are measured in multijet and $t\bar{t}$ + jets samples, separately for b jets and light-quark and gluon jets. These uncertainties affect only the total event yields and are uncorrelated over the years.

The PDF uncertainties are evaluated using the PDF4LHC procedure [58] and the NNPDF3.0 or NNPDF3.1 PDF sets, and are found to change the overall event yields by 0.5–1%. The uncertainty in the measurement of the integrated luminosity amounts to 2.5% [46] for 2016, 2.3% [47] for 2017, and 2.5% [48] for 2018 and affects the normalization of all simulated processes. The uncertainty in the mismodeling of the pileup is evaluated based on a 4.6% variation of the pp total inelastic cross section [59] and affects the normalization of the simulated events. This systematic uncertainty is correlated between the years.

The systematic uncertainties in the background estimation are assessed by multiplying the statistical uncertainties

in the transfer function slope parameters by 4 for the transfer function from the 2M1L to the 3M SR and by 3 for the transfer function from the 3M to the 3T SR. These factors cover the differences observed when the weights are computed in a $t\bar{t}$ sample, enriched in heavy-flavor jets, compared to the multijet sample, populated mainly by light-flavor jets, as well as other uncertainties in the b tagging efficiency. These uncertainties are uncorrelated across data-taking years because they are measured in statistically independent data sets.

VII. RESULTS

The shape of the signal is parametrized from simulation as a Gaussian distribution for each generated value of T quark mass and separately for the low- and high-mass selections. The background shape is determined from the 2M1L and 3M SRs using the corresponding transfer functions, while accounting for the potential presence of signal events.

Binned maximum likelihood fits are performed in the five-jet invariant mass distribution in each region including contributions from background and signal, scaled by the signal strength. Systematic uncertainties, described in Sec. VI, are incorporated as nuisance parameters. The fit is performed separately in the tH and tZ channels. Up to 20% reconstructed tH events are misidentified as tZ candidates. For such events, the shape of the signal remains Gaussian, except the five-jet invariant mass distribution is shifted to lower values compared to the tH channel. Combination of these events with the tH is denoted as “all- tH ” channel.

Figure 5 displays the background-only fits in each of the tH channel search regions for the combined 2016, 2017,

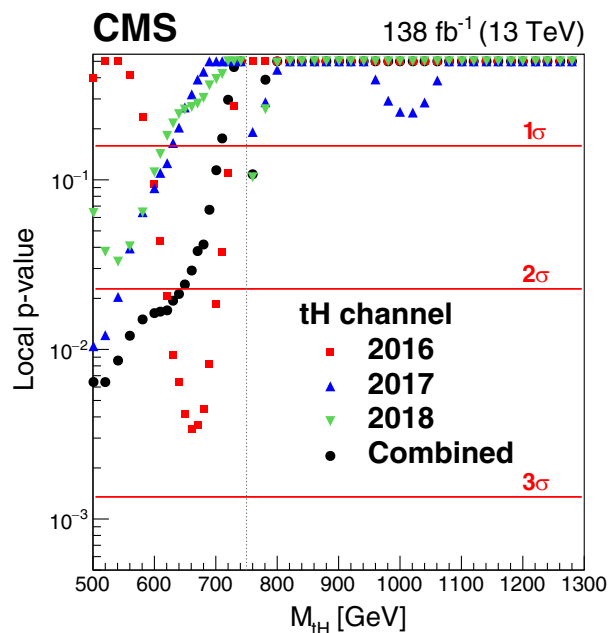


FIG. 6. Observed p -values when considering the tH channel for each year and their combination.

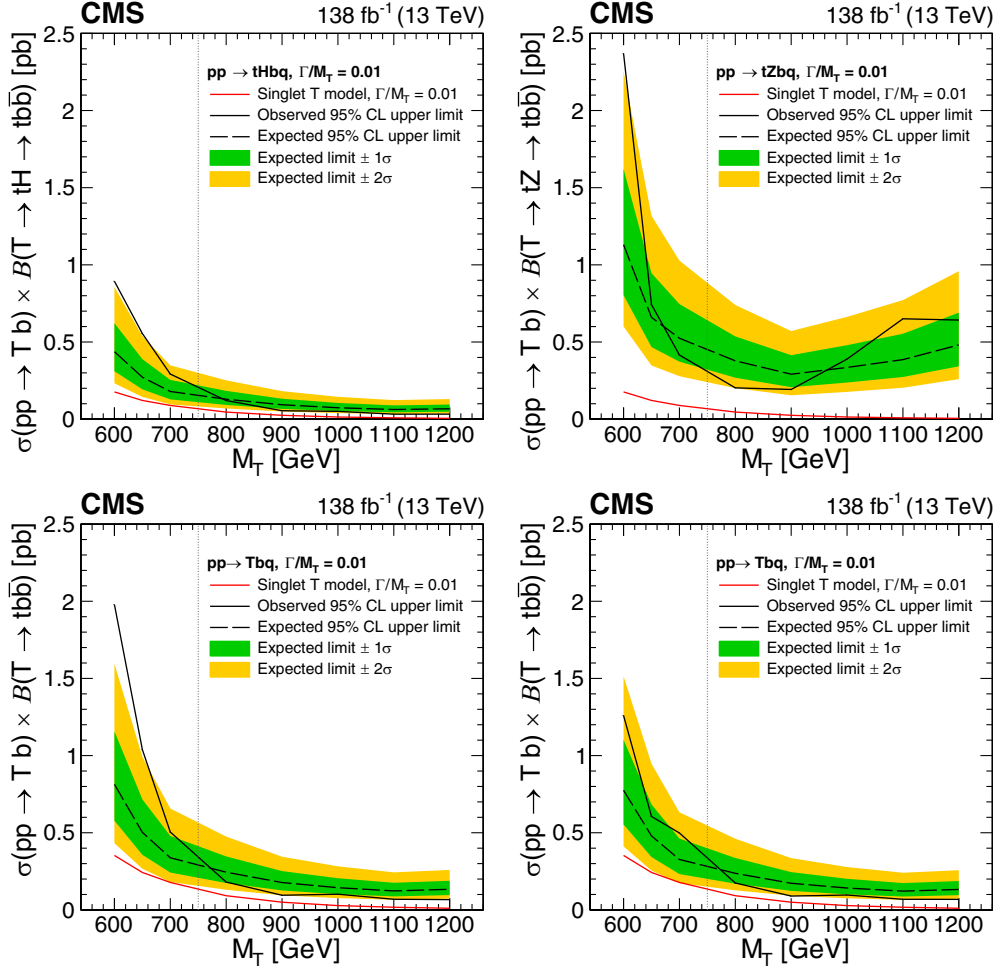


FIG. 7. The observed and expected 95% CL limits on the cross section for associated production with a b quark for final states $tHbq$ (upper left), $tZbq$ (upper right), their sum $tHbq + tZbq$ (lower left), and $tHbq + tZbq$ including the leakage of tH events into the tZ channel (lower right) for different assumed values of the T quark mass. The vertical dashed line represents the crossover point in sensitivity: for masses to the left, the low-mass selection is used to set limits, while for masses to the right, the high-mass selection is used to set limits. The red lines indicate the theoretical cross section for the singlet model [9].

and 2018 data and both the low-mass and high-mass selections. Each figure includes the expected signal distribution for a 700 GeV (low-mass selection) or 900 GeV (high-mass selection) T quark. An upward fluctuation near 680 GeV of the tH spectrum is observed in 2016 data that vanishes once all data-taking years are combined. Figure 6 presents the observed p -values [60].

To evaluate the 95% confidence level (CL) observed and expected limits on the cross section for T quark production, we follow the LHC CL_s criterion [61,62] using the profile likelihood ratio test statistic [63] and the asymptotic formula [64]. The 95% CL upper limits on the cross sections found from the search signatures are derived for T quark masses from 600 to 1200 GeV. The limits are computed for each of the channels: tH , tZ , their combination, and the combination of all- tH channel and tZ channel, as shown in Fig. 7.

For T quark masses above 700 GeV, the observed limits are consistent with the expected ones. Across the full considered T quark mass range of [600,1200] GeV, the narrow-width approximation model cannot be excluded with the current data set. Tabulated results are provided in the HEPData record for this analysis [65].

VIII. SUMMARY

A search for a vectorlike top quark T in the single production mode was performed using proton-proton collision events at $\sqrt{s} = 13$ TeV collected by the CMS experiment in 2016–2018. In this search, the T quark is assumed to couple only to standard model third-generation quarks. We consider signatures containing a top quark and a Higgs (tH) or Z (tZ) boson decaying to a bottom quark-antiquark pair. The major background processes are top

quark-antiquark pair and multijet production. The feature in the tH final state found in the previous search [23] is not confirmed with a larger dataset and improved event selection. No evidence for the T quark production in the $pp \rightarrow Tbq$ process is seen and 95% confidence level upper limits are set on the product of the production cross section and branching fraction to tH and tZ that range from 1260 to 68 fb for T quark masses of 600–1200 GeV. The limits are stronger than those in the previous search by at least a factor of three.

ACKNOWLEDGMENTS

We congratulate our colleagues in the CERN accelerator departments for the excellent performance of the LHC and thank the technical and administrative staffs at CERN and at other CMS institutes for their contributions to the success of the CMS effort. In addition, we gratefully acknowledge the computing centers and personnel of the Worldwide LHC Computing Grid and other centers for delivering so effectively the computing infrastructure essential to our analyses. Finally, we acknowledge the enduring support for the construction and operation of the LHC, the CMS detector, and the supporting computing infrastructure provided by the following funding agencies: SC (Armenia), BMBWF and FWF (Austria); FNRS and FWO (Belgium); CNPq, CAPES, FAPERJ, FAPERGS, and FAPESP (Brazil); MES and BNSF (Bulgaria); CERN; CAS, MoST, and NSFC (China); MINCIENCIAS (Colombia); MSES and CSF (Croatia); RIF (Cyprus); SENESCYT (Ecuador); ERC PRG, RVTT3 and MoER TK202 (Estonia); Academy of Finland, MEC, and HIP (Finland); CEA and CNRS/IN2P3 (France); SRNSF (Georgia); BMBF, DFG, and HGF (Germany); GSRI (Greece); NKFIH (Hungary); DAE and DST (India); IPM (Iran); SFI (Ireland); INFN (Italy); MSIP and NRF (Republic of Korea); MES (Latvia); LMTLT (Lithuania); MOE and UM (Malaysia); BUAP, CINVESTAV, CONACYT, LNS, SEP, and UASLP-FAI (Mexico); MOS (Montenegro); MBIE (New Zealand); PAEC (Pakistan); MES and NSC (Poland); FCT (Portugal); MESTD (Serbia); MCIN/AEI and PCTI (Spain); MOSTR (Sri Lanka); Swiss Funding Agencies (Switzerland); MST (Taipei); MHESI and NSTDA (Thailand); TUBITAK and TENMAK (Turkey); NASU (Ukraine); STFC (United Kingdom); DOE and NSF (USA). Individuals have received support from the Marie-Curie program and the European Research Council and Horizon 2020 Grant, Contracts No. 675440, No. 724704, No. 752730, No. 758316, No. 765710, No. 824093, No. 101115353, No. 101002207, and COST Action CA16108 (European Union); the Leventis

Foundation; the Alfred P. Sloan Foundation; the Alexander von Humboldt Foundation; the Science Committee, Project No. 22rl-037 (Armenia); the Belgian Federal Science Policy Office; the Fonds pour la Formation à la Recherche dans l'Industrie et dans l'Agriculture (FRIA-Belgium); the Agentschap voor Innovatie door Wetenschap en Technologie (IWT-Belgium); the F. R. S.-FNRS and FWO (Belgium) under the “Excellence of Science—EOS”—be.h Project No. 30820817; the Beijing Municipal Science & Technology Commission, No. Z191100007219010 and Fundamental Research Funds for the Central Universities (China); the Ministry of Education, Youth and Sports (MEYS) of the Czech Republic; the Shota Rustaveli National Science Foundation, grant FR-22-985 (Georgia); the Deutsche Forschungsgemeinschaft (DFG), under Germany’s Excellence Strategy—EXC 2121 “Quantum Universe”—390833306, and under project number 400140256—GRK2497; the Hellenic Foundation for Research and Innovation (HFRI), Project Number 2288 (Greece); the Hungarian Academy of Sciences, the New National Excellence Program—ÚNKP, the NKFIH research Grants No. 131991, No. 133046, No. 138136, No. 143460, No. 143477, No. 146913, No. 146914, No. 147048, No. 2020-2.2.1-ED-2021-00181, and No. TKP2021-NKTA-64 (Hungary); the Council of Science and Industrial Research, India; ICSC—National Research Center for High Performance Computing, Big Data and Quantum Computing and FAIR—Future Artificial Intelligence Research, funded by the NextGenerationEU program (Italy); the Latvian Council of Science; the Ministry of Education and Science, Project No. 2022/WK/14, and the National Science Center, contracts Opus 2021/41/B/ST2/01369 and 2021/43/B/ST2/01552 (Poland); the Fundação para a Ciência e a Tecnologia, grant CEECIND/01334/2018 (Portugal); the National Priorities Research Program by Qatar National Research Fund; MCIN/AEI/10.13039/501100011033, ERDF “a way of making Europe,” and the Programa Estatal de Fomento de la Investigación Científica y Técnica de Excelencia María de Maeztu, grant MDM-2017-0765 and Programa Severo Ochoa del Principado de Asturias (Spain); the Chulalongkorn Academic into Its 2nd Century Project Advancement Project, and the National Science, Research and Innovation Fund via the Program Management Unit for Human Resources & Institutional Development, Research and Innovation, grant B37G660013 (Thailand); the Kavli Foundation; the Nvidia Corporation; the SuperMicro Corporation; the Welch Foundation, contract C-1845; and the Weston Havens Foundation (USA).

- [1] Y. Okada and L. Panizzi, LHC signatures of vector-like quarks, *Adv. High Energy Phys.* **2013**, 364936 (2013).
- [2] J. A. Aguilar-Saavedra, R. Benbrik, S. Heinemeyer, and M. Pérez-Victoria, Handbook of vectorlike quarks: Mixing and single production, *Phys. Rev. D* **88**, 094010 (2013).
- [3] A. De Simone, O. Matsedonskyi, R. Rattazzi, and A. Wulzer, A first top partner hunter's guide, *J. High Energy Phys.* **04** (2013) 004.
- [4] M. Buchkremer, G. Cacciapaglia, A. Deandrea, and L. Panizzi, Model independent framework for searches of top partners, *Nucl. Phys.* **B876**, 376 (2013).
- [5] A. Djouadi and A. Lenz, Sealing the fate of a fourth generation of fermions, *Phys. Lett. B* **715**, 310 (2012).
- [6] A. Lenz, Constraints on a fourth generation of fermions from Higgs boson searches, *Adv. High Energy Phys.* **2013**, 910275 (2013).
- [7] CMS Collaboration, Combined search for the quarks of a sequential fourth generation, *Phys. Rev. D* **86**, 112003 (2012).
- [8] N. Vignaroli, Early discovery of top partners and test of the Higgs nature, *Phys. Rev. D* **86**, 075017 (2012).
- [9] J. A. Aguilar-Saavedra, Identifying top partners at LHC, *J. High Energy Phys.* **11** (2009) 030.
- [10] CMS Collaboration, Search for pair production of vector-like quarks in the $bWbW$ channel from proton-proton collisions at $\sqrt{s} = 13$ TeV, *Phys. Lett. B* **779**, 82 (2018).
- [11] ATLAS Collaboration, Search for pair production of heavy vector-like quarks decaying into hadronic final states in pp collisions at $\sqrt{s} = 13$ TeV with the ATLAS detector, *Phys. Rev. D* **98**, 092005 (2018).
- [12] ATLAS Collaboration, Search for pair-produced vector-like top and bottom partners in events with large missing transverse momentum in pp collisions with the ATLAS detector, *Eur. Phys. J. C* **83**, 719 (2023).
- [13] CMS Collaboration, Search for pair production of vector-like quarks in leptonic final states in proton-proton collisions at $\sqrt{s} = 13$ TeV, *J. High Energy Phys.* **07** (2023) 020.
- [14] ATLAS Collaboration, Search for pair-production of vector-like quarks in pp collision events at $\sqrt{s} = 13$ TeV with at least one leptonically decaying Z boson and a third-generation quark with the ATLAS detector, *Phys. Lett. B* **843**, 138019 (2023).
- [15] ATLAS Collaboration, Search for single production of vector-like quarks decaying into Wb in pp collisions at $\sqrt{s} = 13$ TeV with the ATLAS detector, *J. High Energy Phys.* **05** (2019) 164.
- [16] ATLAS Collaboration, Search for large missing transverse momentum in association with one top-quark in proton-proton collisions at $\sqrt{s} = 13$ TeV with the ATLAS detector, *J. High Energy Phys.* **05** (2019) 041.
- [17] ATLAS Collaboration, Search for single production of a vectorlike T quark decaying into a Higgs boson and top quark with fully hadronic final states using the ATLAS detector, *Phys. Rev. D* **105**, 092012 (2022).
- [18] CMS Collaboration, Search for single production of vector-like quarks decaying into a b quark and a W boson in proton-proton collisions at $\sqrt{s} = 13$ TeV, *Phys. Lett. B* **772**, 634 (2017).
- [19] CMS Collaboration, Search for single production of a vector-like T quark decaying to a Z boson and a top quark in proton-proton collisions at $\sqrt{s} = 13$ TeV, *Phys. Lett. B* **781**, 574 (2018).
- [20] CMS Collaboration, Search for single production of a vector-like T quark decaying to a top quark and a Z boson in the final state with jets and missing transverse momentum at $\sqrt{s} = 13$ TeV, *J. High Energy Phys.* **05** (2022) 093.
- [21] CMS Collaboration, Search for single production of a heavy vector-like T quark decaying to a Higgs boson and a top quark with a lepton and jets in the final state, *Phys. Lett. B* **771**, 80 (2017).
- [22] CMS Collaboration, Search for electroweak production of a vector-like quark decaying to a top quark and a Higgs boson using boosted topologies in fully hadronic final states, *J. High Energy Phys.* **04** (2017) 136.
- [23] CMS Collaboration, Search for electroweak production of a vector-like T quark using fully hadronic final states, *J. High Energy Phys.* **01** (2020) 036.
- [24] CMS Collaboration, Description and performance of track and primary-vertex reconstruction with the CMS tracker, *J. Instrum.* **9**, P10009 (2014).
- [25] W. Adam *et al.* (CMS Tracker Group), The CMS phase-1 pixel detector upgrade, *J. Instrum.* **16**, P02027 (2021).
- [26] CMS Collaboration, Track impact parameter resolution for the full pseudo-rapidity coverage in the 2017 dataset with the CMS Phase-1 Pixel detector, CMS Detector Performance Summary Report No. CMS-DP-2020-049, 2020.
- [27] CMS Collaboration, Electron and photon reconstruction and identification with the CMS experiment at the CERN LHC, *J. Instrum.* **16**, P05014 (2021).
- [28] CMS Collaboration, ECAL 2016 refined calibration and Run 2 summary plots, CMS Detector Performance Summary Report No. CMS-DP-2020-021, 2020.
- [29] CMS Collaboration, The CMS experiment at the CERN LHC, *J. Instrum.* **3**, S08004 (2008).
- [30] CMS Collaboration, The CMS trigger system, *J. Instrum.* **12**, P01020 (2017).
- [31] CMS Collaboration, Technical proposal for the Phase-II upgrade of the Compact Muon Solenoid, CMS Technical Proposal No. CERN-LHCC-2015-010, CMS-TDR-15-02, 2015.
- [32] CMS Collaboration, Particle-flow reconstruction and global event description with the CMS detector, *J. Instrum.* **12**, P10003 (2017).
- [33] M. Cacciari, G. P. Salam, and G. Soyez, The anti- k_T jet clustering algorithm, *J. High Energy Phys.* **04** (2008) 063.
- [34] M. Cacciari, G. P. Salam, and G. Soyez, FastJet user manual, *Eur. Phys. J. C* **72**, 1896 (2012).
- [35] CMS Collaboration, Pileup mitigation at CMS in 13 TeV data, *J. Instrum.* **15**, P09018 (2020).
- [36] CMS Collaboration, Jet energy scale and resolution in the CMS experiment in pp collisions at 8 TeV, *J. Instrum.* **12**, P02014 (2017).
- [37] CMS Collaboration, Identification of heavy-flavour jets with the CMS detector in pp collisions at 13 TeV, *J. Instrum.* **13**, P05011 (2018).
- [38] J. Alwall, R. Frederix, S. Frixione, V. Hirschi, F. Maltoni, O. Mattelaer, H. S. Shao, T. Stelzer, P. Torrielli, and M. Zaro, The automated computation of tree-level and next-to-leading order differential cross sections, and their matching

- to parton shower simulations, *J. High Energy Phys.* **07** (2014) 079.
- [39] R. L. Workman *et al.* (Particle Data Group), Review of particle physics, *Prog. Theor. Exp. Phys.* **2022**, 083C01 (2022).
- [40] T. Sjöstrand, S. Ask, J. R. Christiansen, R. Corke, N. Desai, P. Ilten, S. Mrenna, S. Prestel, C. O. Rasmussen, and P. Z. Skands, An introduction to PYTHIA 8.2, *Comput. Phys. Commun.* **191**, 159 (2015).
- [41] CMS Collaboration, Event generator tunes obtained from underlying event and multiparton scattering measurements, *Eur. Phys. J. C* **76**, 155 (2016).
- [42] CMS Collaboration, Extraction and validation of a new set of CMS PYTHIA8 tunes from underlying-event measurements, *Eur. Phys. J. C* **80**, 4 (2020).
- [43] R. D. Ball *et al.* (NNPDF Collaboration), Parton distributions for the LHC Run II, *J. High Energy Phys.* **04** (2015) 040.
- [44] R. D. Ball *et al.* (NNPDF Collaboration), Parton distributions from high-precision collider data, *Eur. Phys. J. C* **77**, 663 (2017).
- [45] S. Agostinelli *et al.* (Geant4 Collaboration), Geant4—a simulation toolkit, *Nucl. Instrum. Methods Phys. Res., Sect. A* **506**, 250 (2003).
- [46] CMS Collaboration, Precision luminosity measurement in proton-proton collisions at $\sqrt{s} = 13$ TeV in 2015 and 2016 at CMS, *Eur. Phys. J. C* **81**, 800 (2021).
- [47] CMS Collaboration, CMS luminosity measurements for the 2017 data taking period, Technical Report No. CMS-PAS-LUM-17-004, CERN, 2017, <https://cds.cern.ch/record/2621960>.
- [48] CMS Collaboration, CMS luminosity measurements for the 2018 data taking period, Technical Report CMS-PAS-LUM-18-002, CERN, 2017, <https://cds.cern.ch/record/2676164>.
- [49] P. Nason, A new method for combining NLO QCD with shower Monte Carlo algorithms, *J. High Energy Phys.* **11** (2004) 040.
- [50] S. Frixione, P. Nason, and C. Oleari, Matching NLO QCD computations with parton shower simulations: The POWHEG method, *J. High Energy Phys.* **11** (2007) 070.
- [51] S. Alioli, P. Nason, C. Oleari, and E. Re, A general framework for implementing NLO calculations in shower Monte Carlo programs: The POWHEG BOX, *J. High Energy Phys.* **06** (2010) 043.
- [52] S. Frixione, P. Nason, and G. Ridolfi, A positive-weight next-to-leading-order Monte Carlo for heavy flavour hadroproduction, *J. High Energy Phys.* **09** (2007) 126.
- [53] H. B. Hartanto, B. Jager, L. Reina, and D. Wackerth, Higgs boson production in association with top quarks in the POWHEG BOX, *Phys. Rev. D* **91**, 094003 (2015).
- [54] G. Luisoni, P. Nason, C. Oleari, and F. Tramontano, $HW^\pm/HZ + 0$ and 1 jet at NLO with the POWHEG BOX interfaced to GoSam and their merging within MinLO, *J. High Energy Phys.* **10** (2013) 083.
- [55] A. N. Kolmogorov, Sulla determinazione empirica di una legge di distribuzione, *G. Ist. Ital. Attuari* **4**, 83 (1933).
- [56] N. Smirnov, Table for estimating the goodness of fit of empirical distributions, *Ann. Math. Stat.* **19**, 279 (1948).
- [57] F. E. James, *Statistical Methods in Experimental Physics*; 2nd ed. (World Scientific, Singapore, 2006).
- [58] J. Butterworth *et al.*, PDF4LHC recommendations for LHC Run II, *J. Phys. G* **43**, 023001 (2016).
- [59] CMS Collaboration, Measurement of the inelastic proton-proton cross section at $\sqrt{s} = 13$ TeV, *J. High Energy Phys.* **07** (2018) 161.
- [60] L. Demortier, P values and nuisance parameters, in *Statistical Issues for LHC Physics. Proceedings of the Workshop on Statistical Issues for LHC Physics, PHYSTAT-LHC, Geneva, Switzerland, 2007* (CERN, Geneva, Switzerland, 2008), p. 23.
- [61] T. Junk, Confidence level computation for combining searches with small statistics, *Nucl. Instrum. Methods Phys. Res. Sect. A* **434**, 435 (1999).
- [62] A. L. Read, Presentation of search results: The CL_s technique, *J. Phys. G* **28**, 2693 (2002).
- [63] ATLAS and CMS Collaborations and LHC Higgs Combination Group, Procedure for the LHC Higgs boson search combination in Summer 2011, Technical Report No. CMS-NOTE-2011-005, ATL-PHYS-PUB-2011-11, 2011, <https://cds.cern.ch/record/1379837>.
- [64] G. Cowan, K. Cranmer, E. Gross, and O. Vitells, Asymptotic formulae for likelihood-based tests of new physics, *Eur. Phys. J. C* **71**, 1554 (2011); **73**, 2501 (2013).
- [65] HEPData record for this analysis (2024), [10.17182/hepdata.144172](https://cds.cern.ch/record/144172).

A. Hayrapetyan,¹ A. Tumasyan^{1,b}, W. Adam², J. W. Andrejkovic,² T. Bergauer², S. Chatterjee², K. Damanakis², M. Dragicevic², P. S. Hussain², M. Jeitler^{2,c}, N. Krammer², A. Li², D. Liko², I. Mikulec², J. Schieck^{2,c}, R. Schöfbeck², D. Schwarz², M. Sonawane², S. Templ², W. Waltenberger², C.-E. Wulz^{2,c}, M. R. Darwish^{3,d}, T. Janssen³, P. Van Mechelen³, E. S. Bols⁴, J. D’Hondt⁴, S. Dansana⁴, A. De Moor⁴, M. Delcourt⁴, H. El Faham⁴, S. Lowette⁴, I. Makarenko⁴, D. Müller⁴, A. R. Sahasransu⁴, S. Tavernier⁴, M. Tytgat^{4,e}, G. P. Van Onsem⁴, S. Van Putte⁴, D. Vannerom⁴, B. Clerbaux⁵, G. De Lentdecker⁵, L. Favart⁵, D. Hohov⁵, J. Jaramillo⁵, A. Khalilzadeh⁵, K. Lee⁵, M. Mahdavihorrani⁵, A. Malara⁵, S. Paredes⁵, L. Pétré⁵, N. Postiau⁵, L. Thomas⁵, M. Vanden Bemden⁵, C. Vander Velde⁵, P. Vanlaer⁵, M. De Coen⁶, D. Dobur⁶, Y. Hong⁶, J. Knolle⁶, L. Lambrecht⁶, G. Mestdach⁶, C. Rendón⁶, A. Samalan⁶, K. Skovpen⁶, N. Van Den Bossche⁶, J. van der Linden⁶, L. Wezenbeek⁶, A. Benecke⁷, A. Bethani⁷, G. Bruno⁷, C. Caputo⁷, C. Delaere⁷, I. S. Donertas⁷, A. Giammanco⁷, K. Jaffel⁷, Sa. Jain⁷, V. Lemaître⁷, J. Lidrych⁷, P. Mastrapasqua⁷, K. Mondal⁷

T. T. Tran⁷, S. Wertz⁷, G. A. Alves⁸, E. Coelho⁸, C. Hensel⁸, T. Menezes De Oliveira⁸, A. Moraes⁸,
P. Rebello Teles⁸, M. Soeiro⁸, W. L. Aldá Júnior⁹, M. Alves Gallo Pereira⁹, M. Barroso Ferreira Filho⁹,
H. Brandao Malbouisson⁹, W. Carvalho⁹, J. Chinellato^{9,f}, E. M. Da Costa⁹, G. G. Da Silveira^{9,g},
D. De Jesus Damiao⁹, S. Fonseca De Souza⁹, R. Gomes De Souza⁹, J. Martins^{9,h}, C. Mora Herrera⁹,
K. Mota Amarilo⁹, L. Mundim⁹, H. Nogima⁹, A. Santoro⁹, A. Sznajder⁹, M. Thiel⁹, A. Vilela Pereira⁹,
C. A. Bernardes^{10,g}, L. Calligaris¹⁰, T. R. Fernandez Perez Tomei¹⁰, E. M. Gregores¹⁰, P. G. Mercadante¹⁰,
S. F. Novaes¹⁰, B. Orzari¹⁰, Sandra S. Padula¹⁰, A. Aleksandrov¹¹, G. Antchev¹¹, R. Hadjiiska¹¹, P. Iaydjiev¹¹,
M. Misheva¹¹, M. Shopova¹¹, G. Sultanov¹¹, A. Dimitrov¹², L. Litov¹², B. Pavlov¹², P. Petkov¹², A. Petrov¹²,
E. Shumka¹², S. Keshri¹³, S. Thakur¹³, T. Cheng¹⁴, Q. Guo¹⁴, T. Javaid¹⁴, L. Yuan¹⁴, Z. Hu¹⁵, J. Liu¹⁵,
K. Yi^{15,i,j}, G. M. Chen^{16,k}, H. S. Chen^{16,k}, M. Chen^{16,k}, F. Iemmi¹⁶, C. H. Jiang¹⁶, A. Kapoor^{16,l}, H. Liao¹⁶,
Z.-A. Liu^{16,m}, R. Sharma^{16,n}, J. N. Song^{16,m}, J. Tao¹⁶, C. Wang^{16,k}, J. Wang¹⁶, Z. Wang^{16,k}, H. Zhang¹⁶,
A. Agapitos¹⁷, Y. Ban¹⁷, A. Levin¹⁷, C. Li¹⁷, Q. Li¹⁷, Y. Mao¹⁷, S. J. Qian¹⁷, X. Sun¹⁷, D. Wang¹⁷, H. Yang¹⁷,
L. Zhang¹⁷, C. Zhou¹⁷, Z. You¹⁸, N. Lu¹⁹, G. Bauer^{20,o}, X. Gao^{21,p}, D. Leggat²¹, H. Okawa²¹, Z. Lin²²,
C. Lu²², M. Xiao²², C. Avila²³, D. A. Barbosa Trujillo²³, A. Cabrera²³, C. Florez²³, J. Fraga²³, J. A. Reyes Vega²³,
J. Mejia Guisao²⁴, F. Ramirez²⁴, M. Rodriguez²⁴, J. D. Ruiz Alvarez²⁴, D. Giljanovic²⁵, N. Godinovic²⁵,
D. Lelas²⁵, A. Sculac²⁵, M. Kovac²⁶, T. Sculac^{26,q}, P. Bargassa²⁷, V. Brigljevic²⁷, B. K. Chitroda²⁷,
D. Ferencek²⁷, S. Mishra²⁷, A. Starodumov^{27,r}, T. Susa²⁷, A. Attikis²⁸, K. Christoforou²⁸, S. Konstantinou²⁸,
J. Mousa²⁸, C. Nicolaou²⁸, F. Ptochos²⁸, P. A. Razis²⁸, H. Rykaczewski²⁸, H. Saka²⁸, A. Stepennov²⁸,
M. Finger²⁹, M. Finger Jr.²⁹, A. Kveton²⁹, E. Ayala³⁰, E. Carrera Jarrin³¹, Y. Assran^{32,s,t}, S. Elgammal^{32,t},
M. A. Mahmoud³³, Y. Mohammed³³, K. Ehataht³⁴, M. Kadastik³⁴, T. Lange³⁴, S. Nandan³⁴, C. Nielsen³⁴,
J. Pata³⁴, M. Raidal³⁴, L. Tani³⁴, C. Veelken³⁴, H. Kirschenmann³⁵, K. Osterberg³⁵, M. Voutilainen³⁵,
S. Bharthuar³⁶, E. Brücken³⁶, F. Garcia³⁶, K. T. S. Kallonen³⁶, R. Kinnunen³⁶, T. Lampén³⁶, K. Lassila-Perini³⁶,
S. Lehti³⁶, T. Lindén³⁶, L. Martikainen³⁶, M. Myllymäki³⁶, M. m. Rantanen³⁶, H. Siikonen³⁶, E. Tuominen³⁶,
J. Tuominiemi³⁶, P. Luukka³⁷, H. Petrow³⁷, M. Besancon³⁸, F. Couderc³⁸, M. Dejardin³⁸, D. Denegri³⁸,
J. L. Faure³⁸, F. Ferri³⁸, S. Ganjour³⁸, P. Gras³⁸, G. Hamel de Monchenault³⁸, V. Lohezic³⁸, J. Malcles³⁸,
J. Rander³⁸, A. Rosowsky³⁸, M. Ö. Sahin³⁸, A. Savoy-Navarro^{38,u}, P. Simkina³⁸, M. Titov³⁸, M. Tornago³⁸,
C. Baldenegro Barrera³⁹, F. Beaudette³⁹, A. Buchot Perraguin³⁹, P. Busson³⁹, A. Cappati³⁹, C. Charlot³⁹,
F. Damas³⁹, O. Davignon³⁹, A. De Wit³⁹, B. A. Fontana Santos Alves³⁹, S. Ghosh³⁹, A. Gilbert³⁹,
R. Granier de Cassagnac³⁹, A. Hakimi³⁹, B. Harikrishnan³⁹, L. Kalipoliti³⁹, G. Liu³⁹, J. Motta³⁹, M. Nguyen³⁹,
C. Ochando³⁹, L. Portales³⁹, R. Salerno³⁹, J. B. Sauvan³⁹, Y. Sirois³⁹, A. Tarabini³⁹, E. Vernazza³⁹, A. Zabi³⁹,
A. Zghiche³⁹, J.-L. Agram^{40,v}, J. Andrea⁴⁰, D. Apparú⁴⁰, D. Bloch⁴⁰, J.-M. Brom⁴⁰, E. C. Chabert⁴⁰,
C. Collard⁴⁰, S. Falke⁴⁰, U. Goerlach⁴⁰, C. Grimault⁴⁰, R. Haeberle⁴⁰, A.-C. Le Bihan⁴⁰, M. Meena⁴⁰, G. Saha⁴⁰,
M. A. Sessini⁴⁰, P. Van Hove⁴⁰, S. Beauceron⁴¹, B. Blancon⁴¹, G. Boudoul⁴¹, N. Chanon⁴¹, J. Choi⁴¹,
D. Contardo⁴¹, P. Depasse⁴¹, C. Dozen^{41,w}, H. El Mamouni⁴¹, J. Fay⁴¹, S. Gascon⁴¹, M. Gouzevitch⁴¹,
C. Greenberg⁴¹, G. Grenier⁴¹, B. Ille⁴¹, I. B. Laktineh⁴¹, M. Lethuillier⁴¹, L. Mirabito⁴¹, S. Perries⁴¹, A. Purohit⁴¹,
M. Vander Donckt⁴¹, P. Verdier⁴¹, J. Xiao⁴¹, I. Lomidze⁴², T. Toriashvili^{42,x}, Z. Tsamalaidze^{42,r}, V. Botta⁴³,
L. Feld⁴³, K. Klein⁴³, M. Lipinski⁴³, D. Meuser⁴³, A. Pauls⁴³, N. Röwert⁴³, M. Teroerde⁴³, S. Diekmann⁴⁴,
A. Dodonova⁴⁴, N. Eich⁴⁴, D. Eliseev⁴⁴, F. Engelke⁴⁴, J. Erdmann⁴⁴, M. Erdmann⁴⁴, P. Fackeldey⁴⁴,
B. Fischer⁴⁴, T. Hebbeker⁴⁴, K. Hoepfner⁴⁴, F. Ivone⁴⁴, A. Jung⁴⁴, M. y. Lee⁴⁴, L. Mastrolorenzo⁴⁴,
F. Mausolf⁴⁴, M. Merschmeyer⁴⁴, A. Meyer⁴⁴, S. Mukherjee⁴⁴, D. Noll⁴⁴, A. Novak⁴⁴, F. Nowotny⁴⁴,
A. Pozdnyakov⁴⁴, Y. Rath⁴⁴, W. Redjeb⁴⁴, F. Rehm⁴⁴, H. Reithler⁴⁴, U. Sarkar⁴⁴, V. Sarkisovi⁴⁴, A. Schmidt⁴⁴,
A. Sharma⁴⁴, J. L. Spahr⁴⁴, A. Stein⁴⁴, F. Torres Da Silva De Araujo^{44,y}, L. Vigilante⁴⁴, S. Wiedenbeck⁴⁴,
S. Zaleski⁴⁴, C. Dziwok⁴⁵, G. Flügge⁴⁵, W. Haj Ahmad^{45,z}, T. Kress⁴⁵, A. Nowack⁴⁵, O. Pooth⁴⁵, A. Stahl⁴⁵,
T. Ziemons⁴⁵, A. Zotz⁴⁵, H. Aarup Petersen⁴⁶, M. Aldaya Martin⁴⁶, J. Alimena⁴⁶, S. Amoroso⁴⁶, Y. An⁴⁶,
S. Baxter⁴⁶, M. Bayatmakou⁴⁶, H. Becerril Gonzalez⁴⁶, O. Behnke⁴⁶, A. Belvedere⁴⁶, S. Bhattacharya⁴⁶,
F. Blekman^{46,aa}, K. Borras^{46,bb}, A. Campbell⁴⁶, A. Cardini⁴⁶, C. Cheng⁴⁶, F. Colombina⁴⁶,
S. Consuegra Rodríguez⁴⁶, G. Correia Silva⁴⁶, M. De Silva⁴⁶, G. Eckerlin⁴⁶, D. Eckstein⁴⁶, L. I. Estevez Banos⁴⁶,
O. Filatov⁴⁶, E. Gallo^{46,aa}, A. Geiser⁴⁶, A. Giralddi⁴⁶, G. Greau⁴⁶, V. Guglielmi⁴⁶, M. Guthoff⁴⁶, A. Hinzmann⁴⁶,
A. Jafari^{46,cc}, L. Jeppe⁴⁶, N. Z. Jomhari⁴⁶, B. Kaech⁴⁶, M. Kasemann⁴⁶, C. Kleinwort⁴⁶, R. Kogler⁴⁶

M. Komm⁴⁶, D. Krücker⁴⁶, W. Lange⁴⁶, D. Leyva Pernia⁴⁶, K. Lipka^{46,dd}, W. Lohmann^{46,ee}, R. Mankel⁴⁶, I.-A. Melzer-Pellmann⁴⁶, M. Mendizabal Morentin⁴⁶, A. B. Meyer⁴⁶, G. Milella⁴⁶, A. Mussgiller⁴⁶, L. P. Nair⁴⁶, A. Nürnberg⁴⁶, Y. Otariid⁴⁶, J. Park⁴⁶, D. Pérez Adán⁴⁶, E. Ranken⁴⁶, A. Raspereza⁴⁶, B. Ribeiro Lopes⁴⁶, J. Rübenach⁴⁶, A. Saggio⁴⁶, M. Scham^{46,ff,bb}, S. Schnake^{46,bb}, P. Schütze⁴⁶, C. Schwanenberger^{46,aa}, D. Selivanova⁴⁶, K. Sharko⁴⁶, M. Shchedrolosiev⁴⁶, R. E. Sosa Ricardo⁴⁶, D. Stafford⁴⁶, F. Vazzoler⁴⁶, A. Ventura Barroso⁴⁶, R. Walsh⁴⁶, Q. Wang⁴⁶, Y. Wen⁴⁶, K. Wichmann⁴⁶, L. Wiens^{46,bb}, C. Wissing⁴⁶, Y. Yang⁴⁶, A. Zimmermann Castro Santos⁴⁶, A. Albrecht⁴⁷, S. Albrecht⁴⁷, M. Antonello⁴⁷, S. Bein⁴⁷, L. Benato⁴⁷, M. Bonanomi⁴⁷, P. Connor⁴⁷, M. Eich⁴⁷, K. El Morabit⁴⁷, Y. Fischer⁴⁷, A. Fröhlich⁴⁷, C. Garbers⁴⁷, E. Garutti⁴⁷, A. Grohsjean⁴⁷, M. Hajheidari⁴⁷, J. Haller⁴⁷, H. R. Jabusch⁴⁷, G. Kasieczka⁴⁷, P. Keicher⁴⁷, R. Klanner⁴⁷, W. Korcari⁴⁷, T. Kramer⁴⁷, V. Kutzner⁴⁷, F. Labe⁴⁷, J. Lange⁴⁷, A. Lobanov⁴⁷, C. Matthies⁴⁷, A. Mehta⁴⁷, L. Moureaux⁴⁷, M. Mrowietz⁴⁷, A. Nigamova⁴⁷, Y. Nissan⁴⁷, A. Paasch⁴⁷, K. J. Pena Rodriguez⁴⁷, T. Quadfasel⁴⁷, B. Raciti⁴⁷, M. Rieger⁴⁷, D. Savoio⁴⁷, J. Schindler⁴⁷, P. Schleper⁴⁷, M. Schröder⁴⁷, J. Schwandt⁴⁷, M. Sommerhalder⁴⁷, H. Stadie⁴⁷, G. Steinbrück⁴⁷, A. Tews⁴⁷, M. Wolf⁴⁷, S. Brommer⁴⁸, M. Burkart⁴⁸, E. Butz⁴⁸, T. Chwalek⁴⁸, A. Dierlamm⁴⁸, A. Droll⁴⁸, N. Faltermann⁴⁸, M. Giffels⁴⁸, A. Gottmann⁴⁸, F. Hartmann^{48,gg}, R. Hofsaess⁴⁸, M. Horzela⁴⁸, U. Husemann⁴⁸, J. Kieseler⁴⁸, M. Klute⁴⁸, R. Koppenhöfer⁴⁸, J. M. Lawhorn⁴⁸, M. Link⁴⁸, A. Lintuluoto⁴⁸, S. Maier⁴⁸, S. Mitra⁴⁸, M. Mormile⁴⁸, Th. Müller⁴⁸, M. Neukum⁴⁸, M. Oh⁴⁸, M. Presilla⁴⁸, G. Quast⁴⁸, K. Rabbertz⁴⁸, B. Regnery⁴⁸, N. Shadskiy⁴⁸, I. Shvetsov⁴⁸, H. J. Simonis⁴⁸, M. Toms^{48,r}, N. Trevisani⁴⁸, R. Ulrich⁴⁸, R. F. Von Cube⁴⁸, M. Wassmer⁴⁸, S. Wieland⁴⁸, F. Wittig⁴⁸, R. Wolf⁴⁸, X. Zuo⁴⁸, G. Anagnostou⁴⁹, G. Daskalakis⁴⁹, A. Kyriakis⁴⁹, A. Papadopoulos^{49,gg}, A. Stakia⁴⁹, P. Kontaxakis⁵⁰, G. Melachroinos⁵⁰, A. Panagiotou⁵⁰, I. Papavergou⁵⁰, I. Paraskevas⁵⁰, N. Saoulidou⁵⁰, K. Theofilatos⁵⁰, E. Tziaferi⁵⁰, K. Vellidis⁵⁰, I. Zisopoulos⁵⁰, G. Bakas⁵¹, T. Chatzistavrou⁵¹, G. Karapostoli⁵¹, K. Kousouris⁵¹, I. Papakrivopoulos⁵¹, E. Siamarkou⁵¹, G. Tsiopolitis⁵¹, A. Zacharopoulou⁵¹, K. Adamidis⁵², I. Bestintzanos⁵², I. Evangelou⁵², C. Foudas⁵², P. Giannios⁵², C. Kamtsikis⁵², P. Katsoulis⁵², P. Kokkas⁵², P. G. Kosmoglou Kioseoglou⁵², N. Manthos⁵², I. Papadopoulos⁵², J. Strologas⁵², M. Bartók^{53,hh}, C. Hajdu⁵³, D. Horvath^{53,ii,jj}, F. Sikler⁵³, V. Veszpremi⁵³, M. Csanád⁵⁴, K. Farkas⁵⁴, M. M. A. Gadallah^{54,kk}, Á. Kadlecik⁵⁴, P. Major⁵⁴, K. Mandal⁵⁴, G. Pásztor⁵⁴, A. J. Rádl^{54,ll}, G. I. Veres⁵⁴, P. Raics⁵⁵, B. Ujvari⁵⁵, G. Zilizi⁵⁵, G. Bencze⁵⁶, S. Czellar⁵⁶, J. Molnar⁵⁶, Z. Szillasi⁵⁶, T. Csorgo^{57,ll}, F. Nemes^{57,ll}, T. Novak⁵⁷, J. Babbar⁵⁸, S. Bansal⁵⁸, S. B. Beri⁵⁸, V. Bhatnagar⁵⁸, G. Chaudhary⁵⁸, S. Chauhan⁵⁸, N. Dhingra^{58,mm}, A. Kaur⁵⁸, A. Kaur⁵⁸, H. Kaur⁵⁸, M. Kaur⁵⁸, S. Kumar⁵⁸, K. Sandeep⁵⁸, T. Sheokand⁵⁸, J. B. Singh⁵⁸, A. Singla⁵⁸, A. Ahmed⁵⁹, A. Bhardwaj⁵⁹, A. Chhetri⁵⁹, B. C. Choudhary⁵⁹, A. Kumar⁵⁹, A. Kumar⁵⁹, M. Naimuddin⁵⁹, K. Ranjan⁵⁹, S. Saumya⁵⁹, S. Baradia⁶⁰, S. Barman^{60,nn}, S. Bhattacharya⁶⁰, S. Dutta⁶⁰, S. Dutta⁶⁰, P. Palit⁶⁰, S. Sarkar⁶⁰, M. M. Ameen⁶¹, P. K. Behera⁶¹, S. C. Behera⁶¹, S. Chatterjee⁶¹, P. Jana⁶¹, P. Kalbhor⁶¹, J. R. Komaragiri^{61,oo}, D. Kumar^{61,oo}, L. Panwar^{61,oo}, P. R. Pujahari⁶¹, N. R. Saha⁶¹, A. Sharma⁶¹, A. K. Sikdar⁶¹, S. Verma⁶¹, S. Dugad⁶², M. Kumar⁶², G. B. Mohanty⁶², P. Suryadevara⁶², A. Bala⁶³, S. Banerjee⁶³, R. M. Chatterjee⁶³, R. K. Dewanjee^{63,pp}, M. Guchait⁶³, Sh. Jain⁶³, S. Karmakar⁶³, S. Kumar⁶³, G. Majumder⁶³, K. Mazumdar⁶³, S. Parolia⁶³, A. Thachayath⁶³, S. Bahinipati^{64,qq}, A. K. Das⁶⁴, C. Kar⁶⁴, D. Maity^{64,rr}, P. Mal⁶⁴, T. Mishra⁶⁴, V. K. Muraleedharan Nair Bindhu^{64,rr}, K. Naskar^{64,rr}, A. Nayak^{64,rr}, P. Sadangi⁶⁴, P. Saha⁶⁴, S. K. Swain⁶⁴, S. Varghese^{64,rr}, D. Vats^{64,rr}, S. Acharya^{65,ss}, A. Alpana⁶⁵, S. Dube⁶⁵, B. Gomber^{65,ss}, B. Kansal⁶⁵, A. Laha⁶⁵, B. Sahu^{65,ss}, S. Sharma⁶⁵, H. Bakhshiansohi^{66,tt}, E. Khazaie^{66,uu}, M. Zeinali^{66,vv}, S. Chenarani^{67,ww}, S. M. Etesami⁶⁷, M. Khakzad⁶⁷, M. Mohammadi Najafabadi⁶⁷, M. Grunewald⁶⁸, M. Abbrescia^{69a,69b}, R. Aly^{69a,69c,xx}, A. Colaleo^{69a,69b}, D. Creanza^{69a,69c}, B. D'Anzi^{69a,69b}, N. De Filippis^{69a,69c}, M. De Palma^{69a,69b}, A. Di Florio^{69a,69c}, W. Elmetenawee^{69a,69b,xx}, L. Fiore^{69a}, G. Iaselli^{69a,69c}, M. Louka^{69a,69b}, G. Maggi^{69a,69c}, M. Maggi^{69a}, I. Margjeka^{69a,69b}, V. Mastrapasqua^{69a,69b}, S. My^{69a,69b}, S. Nuzzo^{69a,69b}, A. Pellecchia^{69a,69b}, A. Pompili^{69a,69b}, G. Pugliese^{69a,69c}, R. Radogna^{69a}, G. Ramirez-Sanchez^{69a,69c}, D. Ramos^{69a}, A. Ranieri^{69a}, L. Silvestris^{69a}, F. M. Simone^{69a,69b}, Ü. Sözbilir^{69a}, A. Stamerra^{69a}, R. Venditti^{69a}, P. Verwilligen^{69a}, A. Zaza^{69a,69b}, G. Abbiendi^{70a}, C. Battilana^{70a,70b}, D. Bonacorsi^{70a,70b}, L. Borgonovi^{70a}, R. Campanini^{70a,70b}, P. Capiluppi^{70a,70b}, A. Castro^{70a,70b}, M. Cuffiani^{70a,70b}, G. M. Dallavalle^{70a}, T. Diotallevi^{70a,70b}, F. Fabbri^{70a}, A. Fanfani^{70a,70b}, D. Fasanella^{70a,70b}, P. Giacomelli^{70a}, L. Giommi^{70a,70b}, C. Grandi^{70a}, L. Guiducci^{70a,70b}, S. Lo Meo^{70a,yy}, L. Lunerti^{70a,70b}, S. Marcellini^{70a}, G. Masetti^{70a}, F. L. Navarra^{70a,70b}

A. Perrotta^{70a} F. Primavera^{70a,70b} A. M. Rossi^{70a,70b} T. Rovelli^{70a,70b} G. P. Siroli^{70a,70b} S. Costa^{71a,71b,zz}
 A. Di Mattia^{71a} R. Potenza^{71a,71b} A. Tricomi^{71a,71b,zz} C. Tuve^{71a,71b} P. Assiouras^{72a} G. Barbagli^{72a}
 G. Bardelli^{72a,72b} B. Camaiani^{72a,72b} A. Cassese^{72a} R. Ceccarelli^{72a} V. Ciulli^{72a,72b} C. Civinini^{72a}
 R. D'Alessandro^{72a,72b} E. Focardi^{72a,72b} T. Kello^{72a} G. Latino^{72a,72b} P. Lenzi^{72a,72b} M. Lizzo^{72a} M. Meschini^{72a}
 S. Paoletti^{72a} A. Papanastassiou^{72a,72b} G. Sguazzoni^{72a} L. Viliani^{72a} L. Benussi⁷³ S. Bianco⁷³ S. Meola^{73,aaa}
 D. Piccolo⁷³ P. Chatagnon^{74a} F. Ferro^{74a} E. Robutti^{74a} S. Tosi^{74a,74b} A. Benaglia^{75a} G. Boldrini^{75a,75b}
 F. Brivio^{75a} F. Cetorelli^{75a} F. De Guio^{75a,75b} M. E. Dinardo^{75a,75b} P. Dini^{75a} S. Gennai^{75a} R. Gerosa^{75a,75b}
 A. Ghezzi^{75a,75b} P. Govoni^{75a,75b} L. Guzzi^{75a} M. T. Lucchini^{75a,75b} M. Malberti^{75a} S. Malvezzi^{75a}
 A. Massironi^{75a} D. Menasce^{75a} L. Moroni^{75a} M. Paganoni^{75a,75b} D. Pedrini^{75a} B. S. Pinolini^{75a}
 S. Ragazzi^{75a,75b} T. Tabarelli de Fatis^{75a,75b} D. Zuolo^{75a} S. Buontempo^{76a} A. Cagnotta^{76a,76b} F. Carnevali^{76a,76b}
 N. Cavallo^{76a,76c} A. De Iorio^{76a,76b} F. Fabozzi^{76a,76c} A. O. M. Iorio^{76a,76b} L. Lista^{76a,76b,bbb} P. Paolucci^{76a,gg}
 B. Rossi^{76a} C. Sciacca^{76a,76b} R. Ardino^{77a} P. Azzi^{77a} N. Bacchetta^{77a,ccc} D. Bisello^{77a,77b} P. Bortignon^{77a}
 A. Bragagnolo^{77a,77b} R. Carlin^{77a,77b} P. Checchia^{77a} T. Dorigo^{77a} U. Gasparini^{77a,77b} E. Lusiani^{77a}
 M. Margoni^{77a,77b} A. T. Meneguzzo^{77a,77b} M. Migliorini^{77a,77b} J. Pazzini^{77a,77b} P. Ronchese^{77a,77b}
 R. Rossin^{77a,77b} M. Sgaravatto^{77a} F. Simonetto^{77a,77b} G. Strong^{77a} M. Tosi^{77a,77b} A. Triossi^{77a,77b}
 S. Ventura^{77a} H. Yarar^{77a,77b} M. Zanetti^{77a,77b} P. Zotto^{77a,77b} A. Zucchetta^{77a,77b} G. Zumerle^{77a,77b}
 S. Abu Zeid^{78a,ddd} C. Aimè^{78a,78b} A. Braghieri^{78a} S. Calzaferri^{78a} D. Fiorina^{78a} P. Montagna^{78a,78b} V. Re^{78a}
 C. Riccardi^{78a,78b} P. Salvini^{78a} I. Vai^{78a,78b} P. Vitulo^{78a,78b} S. Ajmal^{79a,79b} P. Asenov^{79a,eee} G. M. Bilei^{79a}
 D. Ciangottini^{79a,79b} L. Fanò^{79a,79b} M. Magherini^{79a,79b} G. Mantovani^{79a,79b} V. Mariani^{79a,79b} M. Menichelli^{79a}
 F. Moscatelli^{79a,eee} A. Rossi^{79a,79b} A. Santocchia^{79a,79b} D. Spiga^{79a} T. Tedeschi^{79a,79b} P. Azzurri^{80a}
 G. Bagliesi^{80a} R. Bhattacharya^{80a} L. Bianchini^{80a,80b} T. Boccali^{80a} E. Bossini^{80a} D. Bruschini^{80a,80c}
 R. Castaldi^{80a} M. A. Ciocci^{80a,80b} M. Cipriani^{80a,80b} V. D'Amante^{80a,80d} R. Dell'Orso^{80a} S. Donato^{80a}
 A. Giassi^{80a} F. Ligabue^{80a,80c} D. Matos Figueiredo^{80a} A. Messineo^{80a,80b} M. Musich^{80a,80b} F. Palla^{80a}
 A. Rizzi^{80a,80b} G. Rolandi^{80a,80c} S. Roy Chowdhury^{80a} T. Sarkar^{80a} A. Scribano^{80a} P. Spagnolo^{80a}
 R. Tenchini^{80a} G. Tonelli^{80a,80b} N. Turini^{80a,80d} A. Venturi^{80a} P. G. Verdini^{80a} P. Barria^{81a} M. Campana^{81a,81b}
 F. Cavallari^{81a} L. Cunqueiro Mendez^{81a,81b} D. Del Re^{81a,81b} E. Di Marco^{81a} M. Diemoz^{81a} F. Errico^{81a,81b}
 E. Longo^{81a,81b} P. Meridiani^{81a} J. Mijuskovic^{81a,81b} G. Organtini^{81a,81b} F. Pandolfi^{81a} R. Paramatti^{81a,81b}
 C. Quaranta^{81a,81b} S. Rahatlou^{81a,81b} C. Rovelli^{81a} F. Santanastasio^{81a,81b} L. Soffi^{81a} N. Amapane^{82a,82b}
 R. Arcidiacono^{82a,82c} S. Argiro^{82a,82b} M. Arneodo^{82a,82c} N. Bartosik^{82a} R. Bellan^{82a,82b} A. Bellora^{82a,82b}
 C. Biino^{82a} N. Cartiglia^{82a} M. Costa^{82a,82b} R. Covarelli^{82a,82b} N. Demaria^{82a} L. Finco^{82a} M. Grippo^{82a,82b}
 B. Kiani^{82a,82b} F. Legger^{82a} F. Luongo^{82a,82b} C. Mariotti^{82a} S. Maselli^{82a} A. Mecca^{82a,82b} E. Migliore^{82a,82b}
 M. Monteno^{82a} R. Mulargia^{82a} M. M. Obertino^{82a,82b} G. Ortona^{82a} L. Pacher^{82a,82b} N. Pastrone^{82a}
 M. Pelliccioni^{82a} M. Ruspa^{82a,82c} F. Siviero^{82a,82b} V. Sola^{82a,82b} A. Solano^{82a,82b} A. Staiano^{82a}
 C. Tarricone^{82a,82b} D. Trocino^{82a} G. Umoret^{82a,82b} E. Vlasov^{82a,82b} S. Belforte^{83a} V. Candelise^{83a,83b}
 M. Casarsa^{83a} F. Cossutti^{83a} K. De Leo^{83a,83b} G. Della Ricca^{83a,83b} S. Dogra⁸⁴ J. Hong⁸⁴ C. Huh⁸⁴
 B. Kim⁸⁴ D. H. Kim⁸⁴ J. Kim⁸⁴ H. Lee⁸⁴ S. W. Lee⁸⁴ C. S. Moon⁸⁴ Y. D. Oh⁸⁴ M. S. Ryu⁸⁴ S. Sekmen⁸⁴
 Y. C. Yang⁸⁴ M. S. Kim⁸⁵ G. Bak⁸⁶ P. Gwak⁸⁶ H. Kim⁸⁶ D. H. Moon⁸⁶ E. Asilar⁸⁷ D. Kim⁸⁷ T. J. Kim⁸⁷
 J. A. Merlin⁸⁷ S. Choi⁸⁸ S. Han⁸⁸ B. Hong⁸⁸ K. Lee⁸⁸ K. S. Lee⁸⁸ S. Lee⁸⁸ J. Park⁸⁸ S. K. Park⁸⁸ J. Yoo⁸⁸
 J. Goh⁸⁹ S. Yang⁸⁹ H. S. Kim⁹⁰ Y. Kim⁹⁰ S. Lee⁹⁰ J. Almond⁹¹ J. H. Bhyun⁹¹ J. Choi⁹¹ W. Jun⁹¹ J. Kim⁹¹
 S. Ko⁹¹ H. Kwon⁹¹ H. Lee⁹¹ J. Lee⁹¹ J. Lee⁹¹ B. H. Oh⁹¹ S. B. Oh⁹¹ H. Seo⁹¹ U. K. Yang⁹¹ I. Yoon⁹¹
 W. Jang⁹² D. Y. Kang⁹² Y. Kang⁹² S. Kim⁹² B. Ko⁹² J. S. H. Lee⁹² Y. Lee⁹² I. C. Park⁹² Y. Roh⁹²
 I. J. Watson⁹² S. Ha⁹³ H. D. Yoo⁹³ M. Choi⁹⁴ M. R. Kim⁹⁴ H. Lee⁹⁴ Y. Lee⁹⁴ I. Yu⁹⁴ T. Beyrouthy⁹⁵
 Y. Maghrbi⁹⁵ K. Dreimanis⁹⁶ A. Gaile⁹⁶ G. Pikurs⁹⁶ A. Potrebko⁹⁶ M. Seidel⁹⁶ V. Veckalns^{96,fff}
 N. R. Strautnieks⁹⁷ M. Ambrozias⁹⁸ A. Juodagalvis⁹⁸ A. Rinkevicius⁹⁸ G. Tamulaitis⁹⁸
 N. Bin Norjoharuddeen⁹⁹ I. Yusuff^{99,ggg} Z. Zolkapli⁹⁹ J. F. Benitez¹⁰⁰ A. Castaneda Hernandez¹⁰⁰
 H. A. Encinas Acosta¹⁰⁰ L. G. Gallegos Maríñez¹⁰⁰ M. León Coello¹⁰⁰ J. A. Murillo Quijada¹⁰⁰ A. Sehrawat¹⁰⁰
 L. Valencia Palomo¹⁰⁰ G. Ayala¹⁰¹ H. Castilla-Valdez¹⁰¹ E. De La Cruz-Burelo¹⁰¹ I. Heredia-De La Cruz^{101,hhh}
 R. Lopez-Fernandez¹⁰¹ C. A. Mondragon Herrera¹⁰¹ A. Sánchez Hernández¹⁰¹ C. Oropeza Barrera¹⁰²
 M. Ramírez García¹⁰² I. Bautista¹⁰³ I. Pedraza¹⁰³ H. A. Salazar Ibarguen¹⁰³ C. Uribe Estrada¹⁰³ I. Bujanja¹⁰⁴

N. Raicevic¹⁰⁴ P. H. Butler¹⁰⁵ A. Ahmad¹⁰⁶ M. I. Asghar¹⁰⁶ A. Awais¹⁰⁶ M. I. M. Awan¹⁰⁶ H. R. Hoorani¹⁰⁶
W. A. Khan¹⁰⁶ V. Avati¹⁰⁷ L. Grzanka¹⁰⁷ M. Malawski¹⁰⁷ H. Bialkowska¹⁰⁸ M. Bluj¹⁰⁸ B. Boimska¹⁰⁸
M. Górski¹⁰⁸ M. Kazana¹⁰⁸ M. Szeleper¹⁰⁸ P. Zalewski¹⁰⁸ K. Bunkowski¹⁰⁹ K. Doroba¹⁰⁹ A. Kalinowski¹⁰⁹
M. Konecki¹⁰⁹ J. Krolikowski¹⁰⁹ A. Muhammad¹⁰⁹ K. Pozniak¹¹⁰ W. Zabolotny¹¹⁰ M. Araujo¹¹¹
D. Bastos¹¹¹ C. Beirão Da Cruz E Silva¹¹¹ A. Boletti¹¹¹ M. Bozzo¹¹¹ T. Camporesi¹¹¹ G. Da Molin¹¹¹
P. Faccioli¹¹¹ M. Gallinaro¹¹¹ J. Hollar¹¹¹ N. Leonardo¹¹¹ T. Niknejad¹¹¹ A. Petrilli¹¹¹ M. Pisano¹¹¹
J. Seixas¹¹¹ J. Varela¹¹¹ J. W. Wulff¹¹¹ P. Adzic¹¹² P. Milenovic¹¹² M. Dordevic¹¹³ J. Milosevic¹¹³
V. Rekovic¹¹³ M. Aguilar-Benitez¹¹⁴ J. Alcaraz Maestre¹¹⁴ Cristina F. Bedoya¹¹⁴ M. Cepeda¹¹⁴ M. Cerrada¹¹⁴
N. Colino¹¹⁴ B. De La Cruz¹¹⁴ A. Delgado Peris¹¹⁴ A. Escalante Del Valle¹¹⁴ D. Fernández Del Val¹¹⁴
J. P. Fernández Ramos¹¹⁴ J. Flix¹¹⁴ M. C. Fouz¹¹⁴ O. Gonzalez Lopez¹¹⁴ S. Goy Lopez¹¹⁴ J. M. Hernandez¹¹⁴
M. I. Josa¹¹⁴ D. Moran¹¹⁴ C. M. Morcillo Perez¹¹⁴ Á. Navarro Tobar¹¹⁴ C. Perez Dengra¹¹⁴
A. Pérez-Calero Yzquierdo¹¹⁴ J. Puerta Pelayo¹¹⁴ I. Redondo¹¹⁴ D. D. Redondo Ferrero¹¹⁴ L. Romero¹¹⁴
S. Sánchez Navas¹¹⁴ L. Urda Gómez¹¹⁴ J. Vazquez Escobar¹¹⁴ C. Willmott¹¹⁴ J. F. de Trocóniz¹¹⁵
B. Alvarez Gonzalez¹¹⁶ J. Cuevas¹¹⁶ J. Fernandez Menendez¹¹⁶ S. Folgueras¹¹⁶ I. Gonzalez Caballero¹¹⁶
J. R. González Fernández¹¹⁶ E. Palencia Cortezon¹¹⁶ C. Ramón Álvarez¹¹⁶ V. Rodríguez Bouza¹¹⁶
A. Soto Rodríguez¹¹⁶ A. Trapote¹¹⁶ C. Vico Villalba¹¹⁶ P. Vischia¹¹⁶ S. Bhowmik¹¹⁷ S. Blanco Fernández¹¹⁷
J. A. Brochero Cifuentes¹¹⁷ I. J. Cabrillo¹¹⁷ A. Calderon¹¹⁷ J. Duarte Campderros¹¹⁷ M. Fernandez¹¹⁷
G. Gomez¹¹⁷ C. Lasaosa García¹¹⁷ C. Martinez Rivero¹¹⁷ P. Martinez Ruiz del Arbol¹¹⁷ F. Matorras¹¹⁷
P. Matorras Cuevas¹¹⁷ E. Navarrete Ramos¹¹⁷ J. Piedra Gomez¹¹⁷ L. Scodellaro¹¹⁷ I. Vila¹¹⁷
J. M. Vizan Garcia¹¹⁷ M. K. Jayananda¹¹⁸ B. Kailasapathy^{118,iii} D. U. J. Sonnadara¹¹⁸
D. D. C. Wickramaratna¹¹⁸ W. G. D. Dharmaratna^{119,iii} K. Liyanage¹¹⁹ N. Perera¹¹⁹ N. Wickramage¹¹⁹
D. Abbaneo¹²⁰ C. Amendola¹²⁰ E. Auffray¹²⁰ G. Auzinger¹²⁰ J. Baechler¹²⁰ D. Barney¹²⁰
A. Bermúdez Martínez¹²⁰ M. Bianco¹²⁰ B. Bilin¹²⁰ A. A. Bin Anuar¹²⁰ A. Bocci¹²⁰ C. Botta¹²⁰
E. Brondolin¹²⁰ C. Caillol¹²⁰ G. Cerminara¹²⁰ N. Chernyavskaya¹²⁰ D. d'Enterria¹²⁰ A. Dabrowski¹²⁰
A. David¹²⁰ A. De Roeck¹²⁰ M. M. Defranichis¹²⁰ M. Deile¹²⁰ M. Dobson¹²⁰ L. Forthomme¹²⁰
G. Franzoni¹²⁰ W. Funk¹²⁰ S. Giani¹²⁰ D. Gigi¹²⁰ K. Gill¹²⁰ F. Glege¹²⁰ L. Gouskos¹²⁰ M. Haranko¹²⁰
J. Hegeman¹²⁰ B. Huber¹²⁰ V. Innocente¹²⁰ T. James¹²⁰ P. Janot¹²⁰ S. Laurila¹²⁰ P. Lecoq¹²⁰ E. Leutgeb¹²⁰
C. Lourenço¹²⁰ B. Maier¹²⁰ L. Malgeri¹²⁰ M. Mannelli¹²⁰ A. C. Marini¹²⁰ M. Matthewman¹²⁰ F. Meijers¹²⁰
S. Mersi¹²⁰ E. Meschi¹²⁰ V. Milosevic¹²⁰ F. Monti¹²⁰ F. Moortgat¹²⁰ M. Mulders¹²⁰ I. Neutelings¹²⁰
S. Orfanelli¹²⁰ F. Pantaleo¹²⁰ G. Petrucciani¹²⁰ A. Pfeiffer¹²⁰ M. Pierini¹²⁰ D. Piparo¹²⁰ H. Qu¹²⁰
D. Rabady¹²⁰ G. Reales Gutiérrez¹²⁰ M. Rovere¹²⁰ H. Sakulin¹²⁰ S. Scarfi¹²⁰ C. Schwick¹²⁰ M. Selvaggi¹²⁰
A. Sharma¹²⁰ K. Shchelina¹²⁰ P. Silva¹²⁰ P. Sphicas^{120,kkk} A. G. Stahl Leiton¹²⁰ A. Steen¹²⁰ S. Summers¹²⁰
D. Treille¹²⁰ P. Tropea¹²⁰ A. Tsiros¹²⁰ D. Walter¹²⁰ J. Wanczyk^{120,iii} J. Wang¹²⁰ S. Wuchterl¹²⁰ P. Zehetner¹²⁰
P. Zejdl¹²⁰ W. D. Zeuner¹²⁰ T. Bevilacqua^{121,mmm} L. Caminada^{121,mmm} A. Ebrahimi¹²¹ W. Erdmann¹²¹
R. Horisberger¹²¹ Q. Ingram¹²¹ H. C. Kaestli¹²¹ D. Kotlinski¹²¹ C. Lange¹²¹ M. Missiroli^{121,mmm}
L. Noehte^{121,mmm} T. Rohe¹²¹ T. K. Aarrestad¹²² K. Androsov^{122,iii} M. Backhaus¹²² A. Calandri¹²²
C. Cazzaniga¹²² K. Datta¹²² A. De Cosa¹²² G. Dissertori¹²² M. Dittmar¹²² M. Donegà¹²² F. Eble¹²²
M. Galli¹²² K. Gedia¹²² F. Glessgen¹²² C. Grab¹²² D. Hits¹²² W. Luster mann¹²² A.-M. Lyon¹²²
R. A. Manzoni¹²² M. Marchegiani¹²² L. Marchese¹²² C. Martin Perez¹²² A. Mascellani^{122,iii}
F. Nessi-Tedaldi¹²² F. Pauss¹²² V. Perovic¹²² S. Pigazzini¹²² C. Reissel¹²² T. Reitenspiess¹²² B. Ristic¹²²
F. Riti¹²² D. Ruini¹²² R. Seidita¹²² J. Steggemann^{122,iii} D. Valsecchi¹²² R. Wallny¹²² C. Amsler^{123,nnn}
P. Bäertschi¹²³ D. Brzhechko¹²³ M. F. Canelli¹²³ K. Cormier¹²³ J. K. Heikkilä¹²³ M. Huwiler¹²³ W. Jin¹²³
A. Jofrehei¹²³ B. Kilminster¹²³ S. Leontsinis¹²³ S. P. Liechi¹²³ A. Macchiolo¹²³ P. Meiring¹²³
U. Molinatti¹²³ A. Reimers¹²³ P. Robmann¹²³ S. Sanchez Cruz¹²³ M. Senger¹²³ Y. Takahashi¹²³
R. Tramontano¹²³ C. Adloff^{124,ooo} D. Bhowmik¹²⁴ C. M. Kuo¹²⁴ W. Lin¹²⁴ P. K. Rout¹²⁴ P. C. Tiwari^{124,oo}
S. S. Yu¹²⁴ L. Ceard¹²⁵ Y. Chao¹²⁵ K. F. Chen¹²⁵ P. s. Chen¹²⁵ Z. g. Chen¹²⁵ W.-S. Hou¹²⁵ T. h. Hsu¹²⁵
Y. w. Kao¹²⁵ R. Khurana¹²⁵ G. Kole¹²⁵ Y. y. Li¹²⁵ R.-S. Lu¹²⁵ E. Paganis¹²⁵ X. f. Su¹²⁵ J. Thomas-Wilsker¹²⁵
L. s. Tsai¹²⁵ H. y. Wu¹²⁵ E. Yazgan¹²⁵ C. Asawatangtrakuldee¹²⁶ N. Srimanobhas¹²⁶ V. Wachirapusanand¹²⁶
D. Agyel¹²⁷ F. Boran¹²⁷ Z. S. Demiroglu¹²⁷ F. Dolek¹²⁷ I. Dumanoglu^{127,ppp} E. Eskut¹²⁷ Y. Guler^{127,qqq}

E. Gurpinar Guler^{127,qqq} C. Isik¹²⁷ O. Kara,¹²⁷ A. Kayis Topaksu¹²⁷ U. Kiminsu¹²⁷ G. Onengut¹²⁷
K. Ozdemir^{127,rrr} A. Polatoz¹²⁷ B. Tali^{127,sss} U. G. Tok¹²⁷ S. Turkcapar¹²⁷ E. Uslan¹²⁷ I. S. Zorbakir¹²⁷
M. Yalvac^{128,ttt} B. Akgun¹²⁹ I. O. Atakisi¹²⁹ E. Gülmez¹²⁹ M. Kaya^{129,uuu} O. Kaya^{129,vvv} S. Tekten^{129,www}
A. Cakir¹³⁰ K. Cankocak^{130,ppp,xxx} Y. Komurcu¹³⁰ S. Sen^{130,yyy} O. Aydilek¹³¹ S. Cerci^{131,sss} V. Epshteyn¹³¹
B. Hacisahinoglu¹³¹ I. Hos^{131,zzz} B. Kaynak¹³¹ S. Ozkorucuklu¹³¹ O. Potok¹³¹ H. Sert¹³¹ C. Simsek¹³¹
C. Zorbilmez¹³¹ B. Isildak^{132,aaaa} D. Sunar Cerci^{132,sss} A. Boyaryntsev¹³³ B. Grynyov¹³³ L. Levchuk¹³⁴
D. Anthony¹³⁵ J. J. Brooke¹³⁵ A. Bundock¹³⁵ F. Bury¹³⁵ E. Clement¹³⁵ D. Cussans¹³⁵ H. Flacher¹³⁵
M. Glowacki,¹³⁵ J. Goldstein¹³⁵ H. F. Heath¹³⁵ L. Kreczko¹³⁵ S. Paramesvaran¹³⁵ S. Seif El Nasr-Storey,¹³⁵
V. J. Smith¹³⁵ N. Stylianou^{135,bbbb} K. Walkingshaw Pass,¹³⁵ R. White¹³⁵ A. H. Ball,¹³⁶ K. W. Bell¹³⁶
A. Belyaev^{136,cccc} C. Brew¹³⁶ R. M. Brown¹³⁶ D. J. A. Cockerill¹³⁶ C. Cooke¹³⁶ K. V. Ellis,¹³⁶ K. Harder¹³⁶
S. Harper¹³⁶ M.-L. Holmberg^{136,ddd} J. Linacre¹³⁶ K. Manolopoulos,¹³⁶ D. M. Newbold¹³⁶ E. Olaiya,¹³⁶
D. Petyt¹³⁶ T. Reis¹³⁶ G. Salvi¹³⁶ T. Schuh,¹³⁶ C. H. Shepherd-Themistocleous¹³⁶ I. R. Tomalin¹³⁶
T. Williams¹³⁶ R. Bainbridge¹³⁷ P. Bloch¹³⁷ C. E. Brown¹³⁷ O. Buchmuller,¹³⁷ V. Cacchio,¹³⁷
C. A. Carrillo Montoya¹³⁷ G. S. Chahal^{137,eeee} D. Colling¹³⁷ J. S. Dancu,¹³⁷ I. Das¹³⁷ P. Dauncey¹³⁷
G. Davies¹³⁷ J. Davies,¹³⁷ M. Della Negra¹³⁷ S. Fayer,¹³⁷ G. Fedi¹³⁷ G. Hall¹³⁷ M. H. Hassanshahi¹³⁷
A. Howard,¹³⁷ G. Iles¹³⁷ M. Knight¹³⁷ J. Langford¹³⁷ J. León Holgado¹³⁷ L. Lyons¹³⁷ A.-M. Magnan¹³⁷
S. Malik,¹³⁷ M. Mieskolainen¹³⁷ J. Nash^{137,fff} M. Pesaresi¹³⁷ B. C. Radburn-Smith¹³⁷ A. Richards,¹³⁷ A. Rose¹³⁷
C. Seez¹³⁷ R. Shukla¹³⁷ A. Tapper¹³⁷ K. Uchida¹³⁷ G. P. Uttley¹³⁷ L. H. Vage,¹³⁷ T. Virdee^{137,gg}
M. Vojinovic¹³⁷ N. Wardle¹³⁷ D. Winterbottom¹³⁷ K. Coldham,¹³⁸ J. E. Cole¹³⁸ A. Khan,¹³⁸ P. Kyberd¹³⁸
I. D. Reid¹³⁸ S. Abdullin¹³⁹ A. Brinkerhoff¹³⁹ B. Caraway¹³⁹ J. Dittmann¹³⁹ K. Hatakeyama¹³⁹
J. Hiltbrand¹³⁹ B. McMaster¹³⁹ M. Saunders¹³⁹ S. Sawant¹³⁹ C. Sutantawibul¹³⁹ J. Wilson¹³⁹ R. Bartek¹⁴⁰
A. Dominguez¹⁴⁰ C. Huerta Escamilla,¹⁴⁰ A. E. Simsek¹⁴⁰ R. Uniyal¹⁴⁰ A. M. Vargas Hernandez¹⁴⁰ B. Bam¹⁴¹
R. Chudasama¹⁴¹ S. I. Cooper¹⁴¹ S. V. Gleyzer¹⁴¹ C. U. Perez¹⁴¹ P. Rumerio^{141,gggg} E. Usai¹⁴¹ R. Yi¹⁴¹
A. Akpinar¹⁴² D. Arcaro¹⁴² C. Cosby¹⁴² Z. Demiragli¹⁴² C. Erice¹⁴² C. Fangmeier¹⁴²
C. Fernandez Madrazo¹⁴² E. Fontanesi¹⁴² D. Gastler¹⁴² F. Golf¹⁴² S. Jeon¹⁴² I. Reed¹⁴² J. Rohlf¹⁴²
K. Salyer¹⁴² D. Sperka¹⁴² D. Spitzbart¹⁴² I. Suarez¹⁴² A. Tsatsos¹⁴² S. Yuan¹⁴² A. G. Zecchinelli¹⁴²
G. Benelli¹⁴³ X. Coubez,^{143,bb} D. Cutts¹⁴³ M. Hadley¹⁴³ U. Heintz¹⁴³ J. M. Hogan^{143,hhhh} T. Kwon¹⁴³
G. Landsberg¹⁴³ K. T. Lau¹⁴³ D. Li¹⁴³ J. Luo¹⁴³ S. Mondal¹⁴³ M. Narain^{143,a} N. Pervan¹⁴³ S. Sagir^{143,iiii}
F. Simpson¹⁴³ M. Stamenkovic¹⁴³ W. Y. Wong,¹⁴³ X. Yan¹⁴³ W. Zhang,¹⁴³ S. Abbott¹⁴⁴ J. Bonilla¹⁴⁴
C. Brainerd¹⁴⁴ R. Breedon¹⁴⁴ M. Calderon De La Barca Sanchez¹⁴⁴ M. Chertok¹⁴⁴ M. Citron¹⁴⁴ J. Conway¹⁴⁴
P. T. Cox¹⁴⁴ R. Erbacher¹⁴⁴ F. Jensen¹⁴⁴ O. Kukral¹⁴⁴ G. Mocellin¹⁴⁴ M. Mulhearn¹⁴⁴ D. Pellett¹⁴⁴
W. Wei¹⁴⁴ Y. Yao¹⁴⁴ F. Zhang¹⁴⁴ M. Bachtis¹⁴⁵ R. Cousins¹⁴⁵ A. Datta¹⁴⁵ G. Flores Avila¹⁴⁵ J. Hauser¹⁴⁵
M. Ignatenko¹⁴⁵ M. A. Iqbal¹⁴⁵ T. Lam¹⁴⁵ E. Manca¹⁴⁵ A. Nunez Del Prado,¹⁴⁵ D. Saltzberg¹⁴⁵ V. Valuev¹⁴⁵
R. Clare¹⁴⁶ J. W. Gary¹⁴⁶ M. Gordon,¹⁴⁶ G. Hanson¹⁴⁶ W. Si¹⁴⁶ S. Wimpenny^{146,a} J. G. Branson¹⁴⁷
S. Cittolin¹⁴⁷ S. Cooperstein¹⁴⁷ D. Diaz¹⁴⁷ J. Duarte¹⁴⁷ L. Giannini¹⁴⁷ J. Guiang¹⁴⁷ R. Kansal¹⁴⁷
V. Krutelyov¹⁴⁷ R. Lee¹⁴⁷ J. Letts¹⁴⁷ M. Masciovecchio¹⁴⁷ F. Mokhtar¹⁴⁷ S. Mukherjee¹⁴⁷ M. Pieri¹⁴⁷
M. Quinnan¹⁴⁷ B. V. Sathia Narayanan¹⁴⁷ V. Sharma¹⁴⁷ M. Tadel¹⁴⁷ E. Vourliotis¹⁴⁷ F. Würthwein¹⁴⁷
Y. Xiang¹⁴⁷ A. Yagil¹⁴⁷ A. Barzdukas¹⁴⁸ L. Brennan¹⁴⁸ C. Campagnari¹⁴⁸ A. Dorsett¹⁴⁸ J. Incandela¹⁴⁸
J. Kim¹⁴⁸ A. J. Li¹⁴⁸ P. Masterson¹⁴⁸ H. Mei¹⁴⁸ J. Richman¹⁴⁸ U. Sarica¹⁴⁸ R. Schmitz¹⁴⁸ F. Setti¹⁴⁸
J. Sheplock¹⁴⁸ D. Stuart¹⁴⁸ T. Á. Vámi¹⁴⁸ S. Wang¹⁴⁸ A. Bornheim¹⁴⁹ O. Cerri,¹⁴⁹ A. Latorre,¹⁴⁹ J. Mao¹⁴⁹
H. B. Newman¹⁴⁹ M. Spiropulu¹⁴⁹ J. R. Vlimant¹⁴⁹ C. Wang¹⁴⁹ S. Xie¹⁴⁹ R. Y. Zhu¹⁴⁹ J. Alison¹⁵⁰
S. An¹⁵⁰ M. B. Andrews¹⁵⁰ P. Bryant¹⁵⁰ M. Cremonesi,¹⁵⁰ V. Dutta¹⁵⁰ T. Ferguson¹⁵⁰ A. Harilal¹⁵⁰ C. Liu¹⁵⁰
T. Mudholkar¹⁵⁰ S. Murthy¹⁵⁰ M. Paulini¹⁵⁰ A. Roberts¹⁵⁰ A. Sanchez¹⁵⁰ W. Terrill¹⁵⁰ J. P. Cumalat¹⁵¹
W. T. Ford¹⁵¹ A. Hassani¹⁵¹ G. Karathanasis¹⁵¹ E. MacDonald,¹⁵¹ N. Manganelli¹⁵¹ F. Marini¹⁵¹ A. Perloff¹⁵¹
C. Savard¹⁵¹ N. Schonbeck¹⁵¹ K. Stenson¹⁵¹ K. A. Ulmer¹⁵¹ S. R. Wagner¹⁵¹ N. Zipper¹⁵¹ J. Alexander¹⁵²
S. Bright-Thonney¹⁵² X. Chen¹⁵² D. J. Cranshaw¹⁵² J. Fan¹⁵² X. Fan¹⁵² D. Gadkari¹⁵² S. Hogan¹⁵²
P. Kotamnives,¹⁵² J. Monroy¹⁵² M. Oshiro¹⁵² J. R. Patterson¹⁵² J. Reichert¹⁵² M. Reid¹⁵² A. Ryd¹⁵²
J. Thom¹⁵² P. Wittich¹⁵² R. Zou¹⁵² M. Albrow¹⁵³ M. Alyari¹⁵³ O. Amram¹⁵³ G. Apollinari¹⁵³
A. Apresyan¹⁵³ L. A. T. Bauerdick¹⁵³ D. Berry¹⁵³ J. Berryhill¹⁵³ P. C. Bhat¹⁵³ K. Burkett¹⁵³ J. N. Butler¹⁵³

A. Canepa¹⁵³ G. B. Cerati¹⁵³ H. W. K. Cheung¹⁵³ F. Chlebana¹⁵³ G. Cummings¹⁵³ J. Dickinson¹⁵³
 I. Dutta¹⁵³ V. D. Elvira¹⁵³ Y. Feng¹⁵³ J. Freeman¹⁵³ A. Gandrakota¹⁵³ Z. Gecse¹⁵³ L. Gray¹⁵³ D. Green¹⁵³
 A. Grummer¹⁵³ S. Grünendahl¹⁵³ D. Guerrero¹⁵³ O. Gutsche¹⁵³ R. M. Harris¹⁵³ R. Heller¹⁵³
 T. C. Herwig¹⁵³ J. Hirschauer¹⁵³ L. Horyn¹⁵³ B. Jayatilaka¹⁵³ S. Jindariani¹⁵³ M. Johnson¹⁵³ U. Joshi¹⁵³
 T. Klijnsma¹⁵³ B. Klima¹⁵³ K. H. M. Kwok¹⁵³ S. Lammel¹⁵³ D. Lincoln¹⁵³ R. Lipton¹⁵³ T. Liu¹⁵³
 C. Madrid¹⁵³ K. Maeshima¹⁵³ C. Mantilla¹⁵³ D. Mason¹⁵³ P. McBride¹⁵³ P. Merkel¹⁵³ S. Mrenna¹⁵³
 S. Nahn¹⁵³ J. Ngadiuba¹⁵³ D. Noonan¹⁵³ V. Papadimitriou¹⁵³ N. Pastika¹⁵³ K. Pedro¹⁵³ C. Pena^{153,jjjj}
 F. Ravera¹⁵³ A. Reinsvold Hall^{153,kkkk} L. Ristori¹⁵³ E. Sexton-Kennedy¹⁵³ N. Smith¹⁵³ A. Soha¹⁵³
 L. Spiegel¹⁵³ S. Stoynev¹⁵³ J. Strait¹⁵³ L. Taylor¹⁵³ S. Tkaczyk¹⁵³ N. V. Tran¹⁵³ L. Uplegger¹⁵³
 E. W. Vaandering¹⁵³ I. Zoi¹⁵³ C. Aruta¹⁵⁴ P. Avery¹⁵⁴ D. Bourilkov¹⁵⁴ L. Cadamuro¹⁵⁴ P. Chang¹⁵⁴
 V. Cherepanov¹⁵⁴ R. D. Field¹⁵⁴ E. Koenig¹⁵⁴ M. Kolosova¹⁵⁴ J. Konigsberg¹⁵⁴ A. Korytov¹⁵⁴ K. H. Lo¹⁵⁴
 K. Matchev¹⁵⁴ N. Menendez¹⁵⁴ G. Mitselmakher¹⁵⁴ K. Mohrman¹⁵⁴ A. Muthirakalayil Madhu¹⁵⁴ N. Rawal¹⁵⁴
 D. Rosenzweig¹⁵⁴ S. Rosenzweig¹⁵⁴ K. Shi¹⁵⁴ J. Wang¹⁵⁴ T. Adams¹⁵⁵ A. Al Kadhimi¹⁵⁵ A. Askew¹⁵⁵
 N. Bower¹⁵⁵ R. Habibullah¹⁵⁵ V. Hagopian¹⁵⁵ R. Hashmi¹⁵⁵ R. S. Kim¹⁵⁵ S. Kim¹⁵⁵ T. Kolberg¹⁵⁵
 G. Martinez¹⁵⁵ H. Prosper¹⁵⁵ P. R. Prova¹⁵⁵ M. Wulansatiti¹⁵⁵ R. Yohay¹⁵⁵ J. Zhang¹⁵⁵ B. Alsufyani¹⁵⁶
 M. M. Baarmand¹⁵⁶ S. Butalla¹⁵⁶ T. Elkafray^{156,ddd} M. Hohmann¹⁵⁶ R. Kumar Verma¹⁵⁶ M. Rahmani¹⁵⁶
 E. Yanes¹⁵⁶ M. R. Adams¹⁵⁷ A. Baty¹⁵⁷ C. Bennett¹⁵⁷ R. Cavanaugh¹⁵⁷ R. Escobar Franco¹⁵⁷ O. Evdokimov¹⁵⁷
 C. E. Gerber¹⁵⁷ D. J. Hofman¹⁵⁷ J. h. Lee¹⁵⁷ D. S. Lemos¹⁵⁷ A. H. Merrit¹⁵⁷ C. Mills¹⁵⁷ S. Nanda¹⁵⁷
 G. Oh¹⁵⁷ B. Ozek¹⁵⁷ D. Pilipovic¹⁵⁷ R. Pradhan¹⁵⁷ T. Roy¹⁵⁷ S. Rudrabhatla¹⁵⁷ M. B. Tonjes¹⁵⁷
 N. Varelas¹⁵⁷ Z. Ye¹⁵⁷ J. Yoo¹⁵⁷ M. Alhusseini¹⁵⁸ D. Blend¹⁵⁸ K. Dilsiz^{158,llll} L. Emediato¹⁵⁸ G. Karaman¹⁵⁸
 O. K. Köseyan¹⁵⁸ J.-P. Merlo¹⁵⁸ A. Mestvirishvili^{158,mmmm} J. Nachtman¹⁵⁸ O. Neogi¹⁵⁸ H. Ogul^{158,nnnn}
 Y. Onel¹⁵⁸ A. Penzo¹⁵⁸ C. Snyder¹⁵⁸ E. Tiras^{158,oooo} B. Blumenfeld¹⁵⁹ L. Corcodilos¹⁵⁹ J. Davis¹⁵⁹
 A. V. Gritsan¹⁵⁹ L. Kang¹⁵⁹ S. Kyriacou¹⁵⁹ P. Maksimovic¹⁵⁹ M. Roguljic¹⁵⁹ J. Roskes¹⁵⁹ S. Sekhar¹⁵⁹
 M. Swartz¹⁵⁹ A. Abreu¹⁶⁰ L. F. Alcerro Alcerro¹⁶⁰ J. Anguiano¹⁶⁰ P. Baringer¹⁶⁰ Z. Flowers¹⁶⁰ D. Grove¹⁶⁰
 J. King¹⁶⁰ G. Krintiras¹⁶⁰ M. Lazarovits¹⁶⁰ C. Le Mahieu¹⁶⁰ C. Lindsey¹⁶⁰ J. Marquez¹⁶⁰ N. Minafra¹⁶⁰
 M. Murray¹⁶⁰ M. Nickel¹⁶⁰ M. Pitt¹⁶⁰ S. Popescu^{160,pppp} C. Rogan¹⁶⁰ C. Royon¹⁶⁰ R. Salvatico¹⁶⁰
 S. Sanders¹⁶⁰ C. Smith¹⁶⁰ Q. Wang¹⁶⁰ G. Wilson¹⁶⁰ B. Allmond¹⁶¹ A. Ivanov¹⁶¹ K. Kaadze¹⁶¹
 A. Kalogeropoulos¹⁶¹ D. Kim¹⁶¹ Y. Maravin¹⁶¹ K. Nam¹⁶¹ J. Natoli¹⁶¹ D. Roy¹⁶¹ G. Sorrentino¹⁶¹
 F. Rebassoo¹⁶² D. Wright¹⁶² A. Baden¹⁶³ A. Belloni¹⁶³ Y. M. Chen¹⁶³ S. C. Eno¹⁶³ N. J. Hadley¹⁶³
 S. Jabeen¹⁶³ R. G. Kellogg¹⁶³ T. Koeth¹⁶³ Y. Lai¹⁶³ S. Lascio¹⁶³ A. C. Mignerey¹⁶³ S. Nabili¹⁶³
 C. Palmer¹⁶³ C. Papageorgakis¹⁶³ M. M. Paranjpe¹⁶³ L. Wang¹⁶³ J. Bendavid¹⁶⁴ W. Busza¹⁶⁴ I. A. Cali¹⁶⁴
 M. D'Alfonso¹⁶⁴ J. Eysermans¹⁶⁴ C. Freer¹⁶⁴ G. Gomez-Ceballos¹⁶⁴ M. Goncharov¹⁶⁴ G. Grosso¹⁶⁴ P. Harris¹⁶⁴
 D. Hoang¹⁶⁴ D. Kovalskyi¹⁶⁴ J. Krupa¹⁶⁴ L. Lavezzo¹⁶⁴ Y.-J. Lee¹⁶⁴ K. Long¹⁶⁴ C. Mironov¹⁶⁴ C. Paus¹⁶⁴
 D. Rankin¹⁶⁴ C. Roland¹⁶⁴ G. Roland¹⁶⁴ S. Rothman¹⁶⁴ G. S. F. Stephens¹⁶⁴ Z. Wang¹⁶⁴ B. Wyslouch¹⁶⁴
 T. J. Yang¹⁶⁴ B. Crossman¹⁶⁵ B. M. Joshi¹⁶⁵ C. Kapsiak¹⁶⁵ M. Krohn¹⁶⁵ D. Mahon¹⁶⁵ J. Mans¹⁶⁵
 B. Marzocchi¹⁶⁵ S. Pandey¹⁶⁵ M. Revering¹⁶⁵ R. Rusack¹⁶⁵ R. Saradhy¹⁶⁵ N. Schroeder¹⁶⁵ N. Strobbe¹⁶⁵
 M. A. Wadud¹⁶⁵ L. M. Cremaldi¹⁶⁶ K. Bloom¹⁶⁷ D. R. Claes¹⁶⁷ G. Haza¹⁶⁷ J. Hossain¹⁶⁷ C. Joo¹⁶⁷
 I. Kravchenko¹⁶⁷ J. E. Siado¹⁶⁷ W. Tabb¹⁶⁷ A. Vagnerini¹⁶⁷ A. Wightman¹⁶⁷ F. Yan¹⁶⁷ D. Yu¹⁶⁷
 H. Bandyopadhyay¹⁶⁸ L. Hay¹⁶⁸ I. Iashvili¹⁶⁸ A. Kharchilava¹⁶⁸ M. Morris¹⁶⁸ D. Nguyen¹⁶⁸
 S. Rappoccio¹⁶⁸ H. Rejeb Sfar¹⁶⁸ A. Williams¹⁶⁸ G. Alverson¹⁶⁹ E. Barberis¹⁶⁹ J. Dervan¹⁶⁹ Y. Haddad¹⁶⁹
 Y. Han¹⁶⁹ A. Krishna¹⁶⁹ J. Li¹⁶⁹ M. Lu¹⁶⁹ G. Madigan¹⁶⁹ R. Mccarthy¹⁶⁹ D. M. Morse¹⁶⁹ V. Nguyen¹⁶⁹
 T. Orimoto¹⁶⁹ A. Parker¹⁶⁹ L. Skinnari¹⁶⁹ A. Tishelman-Charny¹⁶⁹ B. Wang¹⁶⁹ D. Wood¹⁶⁹
 S. Bhattacharya¹⁷⁰ J. Bueghly¹⁷⁰ Z. Chen¹⁷⁰ S. Dittmer¹⁷⁰ K. A. Hahn¹⁷⁰ Y. Liu¹⁷⁰ Y. Miao¹⁷⁰
 D. G. Monk¹⁷⁰ M. H. Schmitt¹⁷⁰ A. Taliercio¹⁷⁰ M. Velasco¹⁷⁰ G. Agarwal¹⁷¹ R. Band¹⁷¹ R. Bucci¹⁷¹
 S. Castells¹⁷¹ A. Das¹⁷¹ R. Goldouzian¹⁷¹ M. Hildreth¹⁷¹ K. W. Ho¹⁷¹ K. Hurtado Anampa¹⁷¹ T. Ivanov¹⁷¹
 C. Jessop¹⁷¹ K. Lannon¹⁷¹ J. Lawrence¹⁷¹ N. Loukas¹⁷¹ L. Lutton¹⁷¹ J. Mariano¹⁷¹ N. Marinelli¹⁷¹
 I. Mcalister¹⁷¹ T. McCauley¹⁷¹ C. Mcgrady¹⁷¹ C. Moore¹⁷¹ Y. Musienko^{171,r} H. Nelson¹⁷¹ M. Osherson¹⁷¹
 A. Piccinelli¹⁷¹ R. Ruchti¹⁷¹ A. Townsend¹⁷¹ Y. Wan¹⁷¹ M. Wayne¹⁷¹ H. Yockey¹⁷¹ M. Zarucki¹⁷¹
 L. Zygala¹⁷¹ A. Basnet¹⁷² B. Bylsma¹⁷² M. Carrigan¹⁷² L. S. Durkin¹⁷² C. Hill¹⁷² M. Joyce¹⁷²

M. Nunez Ornelas¹⁷², K. Wei¹⁷², B. L. Winer¹⁷², B. R. Yates¹⁷², F. M. Addesa¹⁷³, H. Bouchamaoui¹⁷³, P. Das¹⁷³, G. Dezoort¹⁷³, P. Elmer¹⁷³, A. Frankenthal¹⁷³, B. Greenberg¹⁷³, N. Haubrich¹⁷³, G. Kopp¹⁷³, S. Kwan¹⁷³, D. Lange¹⁷³, A. Loeliger¹⁷³, D. Marlow¹⁷³, I. Ojalvo¹⁷³, J. Olsen¹⁷³, A. Shevelev¹⁷³, D. Stickland¹⁷³, C. Tully¹⁷³, S. Malik¹⁷⁴, A. S. Bakshi¹⁷⁵, V. E. Barnes¹⁷⁵, S. Chandra¹⁷⁵, R. Chawla¹⁷⁵, S. Das¹⁷⁵, A. Gu¹⁷⁵, L. Gutay¹⁷⁵, M. Jones¹⁷⁵, A. W. Jung¹⁷⁵, D. Kondratyev¹⁷⁵, A. M. Koshy¹⁷⁵, M. Liu¹⁷⁵, G. Negro¹⁷⁵, N. Neumeister¹⁷⁵, G. Paspalaki¹⁷⁵, S. Piperov¹⁷⁵, V. Scheurer¹⁷⁵, J. F. Schulte¹⁷⁵, M. Stojanovic¹⁷⁵, J. Thieman¹⁷⁵, A. K. Virdi¹⁷⁵, F. Wang¹⁷⁵, W. Xie¹⁷⁵, J. Dolen¹⁷⁶, N. Parashar¹⁷⁶, A. Pathak¹⁷⁶, D. Acosta¹⁷⁷, T. Carnahan¹⁷⁷, K. M. Ecklund¹⁷⁷, P. J. Fernández Manteca¹⁷⁷, S. Freed¹⁷⁷, P. Gardner¹⁷⁷, F. J. M. Geurts¹⁷⁷, W. Li¹⁷⁷, O. Miguel Colin¹⁷⁷, B. P. Padley¹⁷⁷, R. Redjimi¹⁷⁷, J. Rotter¹⁷⁷, E. Yigitbasi¹⁷⁷, Y. Zhang¹⁷⁷, A. Bodek¹⁷⁸, P. de Barbaro¹⁷⁸, R. Demina¹⁷⁸, J. L. Dulemba¹⁷⁸, A. Garcia-Bellido¹⁷⁸, O. Hindrichs¹⁷⁸, A. Khukhunaishvili¹⁷⁸, N. Parmar¹⁷⁸, P. Parygin^{178,r}, E. Popova^{178,r}, R. Taus¹⁷⁸, K. Goulianos¹⁷⁹, B. Chiarito¹⁸⁰, J. P. Chou¹⁸⁰, Y. Gershtein¹⁸⁰, E. Halkiadakis¹⁸⁰, A. Hart¹⁸⁰, M. Heindl¹⁸⁰, D. Jaroslawski¹⁸⁰, O. Karacheban^{180,ee}, I. Laflotte¹⁸⁰, A. Lath¹⁸⁰, R. Montalvo¹⁸⁰, K. Nash¹⁸⁰, H. Routray¹⁸⁰, S. Salur¹⁸⁰, S. Schnetzer¹⁸⁰, S. Somalwar¹⁸⁰, R. Stone¹⁸⁰, S. A. Thayil¹⁸⁰, S. Thomas¹⁸⁰, J. Vora¹⁸⁰, H. Wang¹⁸⁰, H. Acharya¹⁸¹, D. Ally¹⁸¹, A. G. Delannoy¹⁸¹, S. Fiorendi¹⁸¹, S. Higginbotham¹⁸¹, T. Holmes¹⁸¹, A. R. Kanuganti¹⁸¹, N. Karunarathna¹⁸¹, L. Lee¹⁸¹, E. Nibigira¹⁸¹, S. Spanier¹⁸¹, D. Aebi¹⁸², M. Ahmad¹⁸², O. Bouhali^{182,qqqq}, R. Eusebi¹⁸², J. Gilmore¹⁸², T. Huang¹⁸², T. Kamon^{182,rrrr}, H. Kim¹⁸², S. Luo¹⁸², R. Mueller¹⁸², D. Overton¹⁸², D. Rathjens¹⁸², A. Safonov¹⁸², N. Akchurin¹⁸³, J. Damgov¹⁸³, V. Hegde¹⁸³, A. Hussain¹⁸³, Y. Kazhykarim¹⁸³, K. Lamichhane¹⁸³, S. W. Lee¹⁸³, A. Mankel¹⁸³, T. Peltola¹⁸³, I. Volobouev¹⁸³, A. Whitbeck¹⁸³, E. Appelt¹⁸⁴, Y. Chen¹⁸⁴, S. Greene¹⁸⁴, A. Gurrola¹⁸⁴, W. Johns¹⁸⁴, R. Kunnawalkam Elayavalli¹⁸⁴, A. Melo¹⁸⁴, F. Romeo¹⁸⁴, P. Sheldon¹⁸⁴, S. Tuo¹⁸⁴, J. Velkovska¹⁸⁴, J. Viinikainen¹⁸⁴, B. Cardwell¹⁸⁵, B. Cox¹⁸⁵, J. Hakala¹⁸⁵, R. Hirosky¹⁸⁵, A. Ledovskoy¹⁸⁵, C. Neu¹⁸⁵, C. E. Perez Lara¹⁸⁵, P. E. Karchin¹⁸⁶, A. Aravind¹⁸⁷, S. Banerjee¹⁸⁷, K. Black¹⁸⁷, T. Bose¹⁸⁷, S. Dasu¹⁸⁷, I. De Bruyn¹⁸⁷, P. Everaerts¹⁸⁷, C. Galloni¹⁸⁷, H. He¹⁸⁷, M. Herndon¹⁸⁷, A. Herve¹⁸⁷, C. K. Koraka¹⁸⁷, A. Lanaro¹⁸⁷, R. Loveless¹⁸⁷, J. Madhusudanan Sreekala¹⁸⁷, A. Mallampalli¹⁸⁷, A. Mohammadi¹⁸⁷, S. Mondal¹⁸⁷, G. Parida¹⁸⁷, D. Pinna¹⁸⁷, A. Savin¹⁸⁷, V. Shang¹⁸⁷, V. Sharma¹⁸⁷, W. H. Smith¹⁸⁷, D. Teague¹⁸⁷, H. F. Tsoi¹⁸⁷, W. Vetens¹⁸⁷, A. Warden¹⁸⁷, S. Afanasiev¹⁸⁸, V. Andreev¹⁸⁸, Yu. Andreev¹⁸⁸, T. Aushev¹⁸⁸, M. Azarkin¹⁸⁸, A. Babaev¹⁸⁸, A. Belyaev¹⁸⁸, V. Blinov^{188,r}, E. Boos¹⁸⁸, V. Borshch¹⁸⁸, D. Budkouski¹⁸⁸, V. Bunichev¹⁸⁸, M. Chadeeva^{188,r}, V. Chekhovsky¹⁸⁸, R. Chistov^{188,r}, A. Dermenev¹⁸⁸, T. Dimova^{188,r}, D. Druzhkin^{188,ssss}, M. Dubinin^{188,jjjj}, L. Dudko¹⁸⁸, G. Gavrilo¹⁸⁸, V. Gavrilo¹⁸⁸, S. Gninenko¹⁸⁸, V. Golovtsov¹⁸⁸, N. Golubev¹⁸⁸, I. Golutvin¹⁸⁸, I. Gorbunov¹⁸⁸, Y. Ivanov¹⁸⁸, V. Kachanov¹⁸⁸, V. Karjavine¹⁸⁸, A. Karneyeu¹⁸⁸, V. Kim^{188,r}, M. Kirakosyan¹⁸⁸, D. Kirpichnikov¹⁸⁸, M. Kirsanov¹⁸⁸, V. Klyukhin¹⁸⁸, O. Kodolova^{188,tttt}, V. Korenkov¹⁸⁸, A. Kozyrev^{188,r}, N. Krasnikov¹⁸⁸, A. Lanev¹⁸⁸, P. Levchenko^{188,uuuu}, N. Lychkovskaya¹⁸⁸, V. Makarenko¹⁸⁸, A. Malakhov¹⁸⁸, V. Matveev^{188,r}, V. Murzin¹⁸⁸, A. Nikitenko^{188,vvvv,tttt}, S. Obraztsov¹⁸⁸, V. Oreshkin¹⁸⁸, V. Palichik¹⁸⁸, V. Perelygin¹⁸⁸, M. Perfilov¹⁸⁸, S. Petrushanko¹⁸⁸, S. Polikarpov^{188,r}, V. Popov¹⁸⁸, O. Radchenko^{188,r}, M. Savina¹⁸⁸, V. Savrin¹⁸⁸, V. Shalae¹⁸⁸, S. Shmatov¹⁸⁸, S. Shulha¹⁸⁸, Y. Skovpen^{188,r}, S. Slabospitskii¹⁸⁸, V. Smirnov¹⁸⁸, D. Sosnov¹⁸⁸, V. Sulimov¹⁸⁸, E. Tcherniaev¹⁸⁸, A. Terkulov¹⁸⁸, O. Teryaev¹⁸⁸, I. Tlisova¹⁸⁸, A. Toropin¹⁸⁸, L. Uvarov¹⁸⁸, A. Uzunian¹⁸⁸, P. Volkov¹⁸⁸, A. Vorobyev^{188,a}, G. Vorotnikov¹⁸⁸, N. Voytishin¹⁸⁸, B. S. Yuldashev^{188,wwww}, A. Zarubin¹⁸⁸, I. Zhizhin¹⁸⁸, and A. Zhokin¹⁸⁸

(CMS Collaboration)

¹Yerevan Physics Institute, Yerevan, Armenia

²Institut für Hochenergiephysik, Vienna, Austria

³Universiteit Antwerpen, Antwerpen, Belgium

⁴Vrije Universiteit Brussel, Brussel, Belgium

⁵Université Libre de Bruxelles, Bruxelles, Belgium

⁶Ghent University, Ghent, Belgium

⁷Université Catholique de Louvain, Louvain-la-Neuve, Belgium

⁸Centro Brasileiro de Pesquisas Físicas, Rio de Janeiro, Brazil

⁹Universidade do Estado do Rio de Janeiro, Rio de Janeiro, Brazil

- ¹⁰*Universidade Estadual Paulista, Universidade Federal do ABC, São Paulo, Brazil*
- ¹¹*Institute for Nuclear Research and Nuclear Energy, Bulgarian Academy of Sciences, Sofia, Bulgaria*
- ¹²*University of Sofia, Sofia, Bulgaria*
- ¹³*Instituto De Alta Investigación, Universidad de Tarapacá, Casilla 7 D, Arica, Chile*
- ¹⁴*Beihang University, Beijing, China*
- ¹⁵*Department of Physics, Tsinghua University, Beijing, China*
- ¹⁶*Institute of High Energy Physics, Beijing, China*
- ¹⁷*State Key Laboratory of Nuclear Physics and Technology, Peking University, Beijing, China*
- ¹⁸*Sun Yat-Sen University, Guangzhou, China*
- ¹⁹*University of Science and Technology of China, Hefei, China*
- ²⁰*Nanjing Normal University, Nanjing, China*
- ²¹*Institute of Modern Physics and Key Laboratory of Nuclear Physics and Ion-beam Application (MOE)—Fudan University, Shanghai, China*
- ²²*Zhejiang University, Hangzhou, Zhejiang, China*
- ²³*Universidad de Los Andes, Bogota, Colombia*
- ²⁴*Universidad de Antioquia, Medellin, Colombia*
- ²⁵*University of Split, Faculty of Electrical Engineering, Mechanical Engineering and Naval Architecture, Split, Croatia*
- ²⁶*University of Split, Faculty of Science, Split, Croatia*
- ²⁷*Institute Rudjer Boskovic, Zagreb, Croatia*
- ²⁸*University of Cyprus, Nicosia, Cyprus*
- ²⁹*Charles University, Prague, Czech Republic*
- ³⁰*Escuela Politecnica Nacional, Quito, Ecuador*
- ³¹*Universidad San Francisco de Quito, Quito, Ecuador*
- ³²*Academy of Scientific Research and Technology of the Arab Republic of Egypt, Egyptian Network of High Energy Physics, Cairo, Egypt*
- ³³*Center for High Energy Physics (CHEP-FU), Fayoum University, El-Fayoum, Egypt*
- ³⁴*National Institute of Chemical Physics and Biophysics, Tallinn, Estonia*
- ³⁵*Department of Physics, University of Helsinki, Helsinki, Finland*
- ³⁶*Helsinki Institute of Physics, Helsinki, Finland*
- ³⁷*Lappeenranta-Lahti University of Technology, Lappeenranta, Finland*
- ³⁸*IRFU, CEA, Université Paris-Saclay, Gif-sur-Yvette, France*
- ³⁹*Laboratoire Leprince-Ringuet, CNRS/IN2P3, Ecole Polytechnique, Institut Polytechnique de Paris, Palaiseau, France*
- ⁴⁰*Université de Strasbourg, CNRS, IPHC UMR 7178, Strasbourg, France*
- ⁴¹*Institut de Physique des 2 Infinis de Lyon (IP2I), Villeurbanne, France*
- ⁴²*Georgian Technical University, Tbilisi, Georgia*
- ⁴³*RWTH Aachen University, I. Physikalisches Institut, Aachen, Germany*
- ⁴⁴*RWTH Aachen University, III. Physikalisches Institut A, Aachen, Germany*
- ⁴⁵*RWTH Aachen University, III. Physikalisches Institut B, Aachen, Germany*
- ⁴⁶*Deutsches Elektronen-Synchrotron, Hamburg, Germany*
- ⁴⁷*University of Hamburg, Hamburg, Germany*
- ⁴⁸*Karlsruher Institut fuer Technologie, Karlsruhe, Germany*
- ⁴⁹*Institute of Nuclear and Particle Physics (INPP), NCSR Demokritos, Aghia Paraskevi, Greece*
- ⁵⁰*National and Kapodistrian University of Athens, Athens, Greece*
- ⁵¹*National Technical University of Athens, Athens, Greece*
- ⁵²*University of Ioánnina, Ioánnina, Greece*
- ⁵³*HUN-REN Wigner Research Centre for Physics, Budapest, Hungary*
- ⁵⁴*MTA-ELTE Lendület CMS Particle and Nuclear Physics Group, Eötvös Loránd University, Budapest, Hungary*
- ⁵⁵*Faculty of Informatics, University of Debrecen, Debrecen, Hungary*
- ⁵⁶*Institute of Nuclear Research ATOMKI, Debrecen, Hungary*
- ⁵⁷*Karoly Robert Campus, MATE Institute of Technology, Gyongyos, Hungary*
- ⁵⁸*Panjab University, Chandigarh, India*
- ⁵⁹*University of Delhi, Delhi, India*
- ⁶⁰*Saha Institute of Nuclear Physics, HBNI, Kolkata, India*
- ⁶¹*Indian Institute of Technology Madras, Madras, India*
- ⁶²*Tata Institute of Fundamental Research-A, Mumbai, India*
- ⁶³*Tata Institute of Fundamental Research-B, Mumbai, India*

- ⁶⁴*National Institute of Science Education and Research, An OCC of Homi Bhabha National Institute, Bhubaneswar, Odisha, India*
- ⁶⁵*Indian Institute of Science Education and Research (IISER), Pune, India*
- ⁶⁶*Isfahan University of Technology, Isfahan, Iran*
- ⁶⁷*Institute for Research in Fundamental Sciences (IPM), Tehran, Iran*
- ⁶⁸*University College Dublin, Dublin, Ireland*
- ⁶⁹*INFN Sezione di Bari, Università di Bari, Politecnico di Bari, Bari, Italy*
- ^{69a}*INFN Sezione di Bari, Bari, Italy*
- ^{69b}*Università di Bari, Bari, Italy*
- ^{69c}*Politecnico di Bari, Bari, Italy*
- ⁷⁰*INFN Sezione di Bologna, Università di Bologna, Bologna, Italy*
- ^{70a}*INFN Sezione di Bologna, Bologna, Italy*
- ^{70b}*Università di Bologna, Bologna, Italy*
- ⁷¹*INFN Sezione di Catania, Università di Catania, Catania, Italy*
- ^{71a}*INFN Sezione di Catania, Catania, Italy*
- ^{71b}*Università di Catania, Catania, Italy*
- ⁷²*INFN Sezione di Firenze, Università di Firenze, Firenze, Italy*
- ^{72a}*INFN Sezione di Firenze, Firenze, Italy*
- ^{72b}*Università di Firenze, Firenze, Italy*
- ⁷³*INFN Laboratori Nazionali di Frascati, Frascati, Italy*
- ⁷⁴*INFN Sezione di Genova, Università di Genova, Genova, Italy*
- ^{74a}*INFN Sezione di Genova, Genova, Italy*
- ^{74b}*Università di Genova, Genova, Italy*
- ⁷⁵*INFN Sezione di Milano-Bicocca, Università di Milano-Bicocca, Milano, Italy*
- ^{75a}*INFN Sezione di Milano-Bicocca, Milano, Italy*
- ^{75b}*Università di Milano-Bicocca, Milano, Italy*
- ⁷⁶*INFN Sezione di Napoli, Università di Napoli 'Federico II', Napoli, Italy, Università della Basilicata, Potenza, Italy, Scuola Superiore Meridionale (SSM), Napoli, Italy*
- ^{76a}*INFN Sezione di Napoli, Napoli, Italy*
- ^{76b}*Università di Napoli 'Federico II', Napoli, Italy*
- ^{76c}*Università della Basilicata, Potenza, Italy*
- ^{76d}*Scuola Superiore Meridionale (SSM), Napoli, Italy*
- ⁷⁷*INFN Sezione di Padova, Università di Padova, Padova, Italy, Università di Trento, Trento, Italy*
- ^{77a}*INFN Sezione di Padova, Padova, Italy*
- ^{77b}*Università di Padova, Padova, Italy*
- ^{77c}*Università di Trento, Trento, Italy*
- ⁷⁸*INFN Sezione di Pavia, Università di Pavia, Pavia, Italy*
- ^{78a}*INFN Sezione di Pavia, Pavia, Italy*
- ^{78b}*Università di Pavia, Pavia, Italy*
- ⁷⁹*INFN Sezione di Perugia, Università di Perugia, Perugia, Italy*
- ^{79a}*INFN Sezione di Perugia, Perugia, Italy*
- ^{79b}*Università di Perugia, Perugia, Italy*
- ⁸⁰*INFN Sezione di Pisa, Università di Pisa, Scuola Normale Superiore di Pisa, Pisa Italy, Università di Siena, Siena, Italy*
- ^{80a}*INFN Sezione di Pisa, Pisa, Italy*
- ^{80b}*Università di Pisa, Pisa, Italy*
- ^{80c}*Scuola Normale Superiore di Pisa, Pisa, Italy*
- ^{80d}*Università di Siena, Siena, Italy*
- ⁸¹*INFN Sezione di Roma, Sapienza Università di Roma, Roma, Italy*
- ^{81a}*INFN Sezione di Roma, Roma, Italy*
- ^{81b}*Sapienza Università di Roma, Roma, Italy*
- ⁸²*INFN Sezione di Torino, Università di Torino, Torino, Italy, Università del Piemonte Orientale, Novara, Italy*
- ^{82a}*INFN Sezione di Torino, Torino, Italy*
- ^{82b}*Università di Torino, Torino, Italy*
- ^{82c}*Università del Piemonte Orientale, Novara, Italy*
- ⁸³*INFN Sezione di Trieste, Università di Trieste, Trieste, Italy*
- ^{83a}*INFN Sezione di Trieste, Trieste, Italy*
- ^{83b}*Università di Trieste, Trieste, Italy*
- ⁸⁴*Kyungpook National University, Daegu, Korea*

- ⁸⁵*Department of Mathematics and Physics—GWNu, Gangneung, Korea*
- ⁸⁶*Chonnam National University, Institute for Universe and Elementary Particles, Kwangju, Korea*
- ⁸⁷*Hanyang University, Seoul, Korea*
- ⁸⁸*Korea University, Seoul, Korea*
- ⁸⁹*Kyung Hee University, Department of Physics, Seoul, Korea*
- ⁹⁰*Sejong University, Seoul, Korea*
- ⁹¹*Seoul National University, Seoul, Korea*
- ⁹²*University of Seoul, Seoul, Korea*
- ⁹³*Yonsei University, Department of Physics, Seoul, Korea*
- ⁹⁴*Sungkyunkwan University, Suwon, Korea*
- ⁹⁵*College of Engineering and Technology, American University of the Middle East (AUM),
Dasman, Kuwait*
- ⁹⁶*Riga Technical University, Riga, Latvia*
- ⁹⁷*University of Latvia (LU), Riga, Latvia*
- ⁹⁸*Vilnius University, Vilnius, Lithuania*
- ⁹⁹*National Centre for Particle Physics, Universiti Malaya, Kuala Lumpur, Malaysia*
- ¹⁰⁰*Universidad de Sonora (UNISON), Hermosillo, Mexico*
- ¹⁰¹*Centro de Investigacion y de Estudios Avanzados del IPN, Mexico City, Mexico*
- ¹⁰²*Universidad Iberoamericana, Mexico City, Mexico*
- ¹⁰³*Benemerita Universidad Autonoma de Puebla, Puebla, Mexico*
- ¹⁰⁴*University of Montenegro, Podgorica, Montenegro*
- ¹⁰⁵*University of Canterbury, Christchurch, New Zealand*
- ¹⁰⁶*National Centre for Physics, Quaid-I-Azam University, Islamabad, Pakistan*
- ¹⁰⁷*AGH University of Krakow, Faculty of Computer Science,
Electronics and Telecommunications, Krakow, Poland*
- ¹⁰⁸*National Centre for Nuclear Research, Swierk, Poland*
- ¹⁰⁹*Institute of Experimental Physics, Faculty of Physics, University of Warsaw, Warsaw, Poland*
- ¹¹⁰*Warsaw University of Technology, Warsaw, Poland*
- ¹¹¹*Laboratório de Instrumentação e Física Experimental de Partículas, Lisboa, Portugal*
- ¹¹²*Faculty of Physics, University of Belgrade, Belgrade, Serbia*
- ¹¹³*VINCA Institute of Nuclear Sciences, University of Belgrade, Belgrade, Serbia*
- ¹¹⁴*Centro de Investigaciones Energéticas Medioambientales y Tecnológicas (CIEMAT), Madrid, Spain*
- ¹¹⁵*Universidad Autónoma de Madrid, Madrid, Spain*
- ¹¹⁶*Universidad de Oviedo, Instituto Universitario de Ciencias y Tecnologías Espaciales de Asturias
(ICTEA), Oviedo, Spain*
- ¹¹⁷*Instituto de Física de Cantabria (IFCA), CSIC-Universidad de Cantabria, Santander, Spain*
- ¹¹⁸*University of Colombo, Colombo, Sri Lanka*
- ¹¹⁹*University of Ruhuna, Department of Physics, Matara, Sri Lanka*
- ¹²⁰*CERN, European Organization for Nuclear Research, Geneva, Switzerland*
- ¹²¹*Paul Scherrer Institut, Villigen, Switzerland*
- ¹²²*ETH Zurich—Institute for Particle Physics and Astrophysics (IPA), Zurich, Switzerland*
- ¹²³*Universität Zürich, Zurich, Switzerland*
- ¹²⁴*National Central University, Chung-Li, Taiwan*
- ¹²⁵*National Taiwan University (NTU), Taipei, Taiwan*
- ¹²⁶*High Energy Physics Research Unit, Department of Physics, Faculty of Science, Chulalongkorn
University, Bangkok, Thailand*
- ¹²⁷*Çukurova University, Physics Department, Science and Art Faculty, Adana, Turkey*
- ¹²⁸*Middle East Technical University, Physics Department, Ankara, Turkey*
- ¹²⁹*Bogazici University, Istanbul, Turkey*
- ¹³⁰*Istanbul Technical University, Istanbul, Turkey*
- ¹³¹*Istanbul University, Istanbul, Turkey*
- ¹³²*Yildiz Technical University, Istanbul, Turkey*
- ¹³³*Institute for Scintillation Materials of National Academy of Science of Ukraine, Kharkiv, Ukraine*
- ¹³⁴*National Science Centre, Kharkiv Institute of Physics and Technology, Kharkiv, Ukraine*
- ¹³⁵*University of Bristol, Bristol, United Kingdom*
- ¹³⁶*Rutherford Appleton Laboratory, Didcot, United Kingdom*
- ¹³⁷*Imperial College, London, United Kingdom*
- ¹³⁸*Brunel University, Uxbridge, United Kingdom*
- ¹³⁹*Baylor University, Waco, Texas, USA*
- ¹⁴⁰*Catholic University of America, Washington, DC, USA*

- ¹⁴¹*The University of Alabama, Tuscaloosa, Alabama, USA*
¹⁴²*Boston University, Boston, Massachusetts, USA*
¹⁴³*Brown University, Providence, Rhode Island, USA*
¹⁴⁴*University of California, Davis, Davis, California, USA*
¹⁴⁵*University of California, Los Angeles, California, USA*
¹⁴⁶*University of California, Riverside, Riverside, California, USA*
¹⁴⁷*University of California, San Diego, La Jolla, California, USA*
¹⁴⁸*University of California, Santa Barbara—Department of Physics, Santa Barbara, California, USA*
¹⁴⁹*California Institute of Technology, Pasadena, California, USA*
¹⁵⁰*Carnegie Mellon University, Pittsburgh, Pennsylvania, USA*
¹⁵¹*University of Colorado Boulder, Boulder, Colorado, USA*
¹⁵²*Cornell University, Ithaca, New York, USA*
¹⁵³*Fermi National Accelerator Laboratory, Batavia, Illinois, USA*
¹⁵⁴*University of Florida, Gainesville, Florida, USA*
¹⁵⁵*Florida State University, Tallahassee, Florida, USA*
¹⁵⁶*Florida Institute of Technology, Melbourne, Florida, USA*
¹⁵⁷*University of Illinois Chicago, Chicago, USA, Chicago, USA*
¹⁵⁸*The University of Iowa, Iowa City, Iowa, USA*
¹⁵⁹*Johns Hopkins University, Baltimore, Maryland, USA*
¹⁶⁰*The University of Kansas, Lawrence, Kansas, USA*
¹⁶¹*Kansas State University, Manhattan, Kansas, USA*
¹⁶²*Lawrence Livermore National Laboratory, Livermore, California, USA*
¹⁶³*University of Maryland, College Park, Maryland, USA*
¹⁶⁴*Massachusetts Institute of Technology, Cambridge, Massachusetts, USA*
¹⁶⁵*University of Minnesota, Minneapolis, Minnesota, USA*
¹⁶⁶*University of Mississippi, Oxford, Mississippi, USA*
¹⁶⁷*University of Nebraska-Lincoln, Lincoln, Nebraska, USA*
¹⁶⁸*State University of New York at Buffalo, Buffalo, New York, USA*
¹⁶⁹*Northeastern University, Boston, Massachusetts, USA*
¹⁷⁰*Northwestern University, Evanston, Illinois, USA*
¹⁷¹*University of Notre Dame, Notre Dame, Indiana, USA*
¹⁷²*The Ohio State University, Columbus, Ohio, USA*
¹⁷³*Princeton University, Princeton, New Jersey, USA*
¹⁷⁴*University of Puerto Rico, Mayaguez, Puerto Rico, USA*
¹⁷⁵*Purdue University, West Lafayette, Indiana, USA*
¹⁷⁶*Purdue University Northwest, Hammond, Indiana, USA*
¹⁷⁷*Rice University, Houston, Texas, USA*
¹⁷⁸*University of Rochester, Rochester, New York, USA*
¹⁷⁹*The Rockefeller University, New York, New York, USA*
¹⁸⁰*Rutgers, The State University of New Jersey, Piscataway, New Jersey, USA*
¹⁸¹*University of Tennessee, Knoxville, Tennessee, USA*
¹⁸²*Texas A&M University, College Station, Texas, USA*
¹⁸³*Texas Tech University, Lubbock, Texas, USA*
¹⁸⁴*Vanderbilt University, Nashville, Tennessee, USA*
¹⁸⁵*University of Virginia, Charlottesville, Virginia, USA*
¹⁸⁶*Wayne State University, Detroit, Michigan, USA*
¹⁸⁷*University of Wisconsin—Madison, Madison, Wisconsin, USA*
¹⁸⁸*An institute or international laboratory covered by a cooperation agreement with CERN*

^aDeceased.

^bAlso at Yerevan State University, Yerevan, Armenia.

^cAlso at TU Wien, Vienna, Austria.

^dAlso at Institute of Basic and Applied Sciences, Faculty of Engineering, Arab Academy for Science, Technology and Maritime Transport, Alexandria, Egypt.

^eAlso at Ghent University, Ghent, Belgium.

^fAlso at Universidade Estadual de Campinas, Campinas, Brazil.

^gAlso at Federal University of Rio Grande do Sul, Porto Alegre, Brazil.

^hAlso at UFMS, Nova Andradina, Brazil.

ⁱAlso at Nanjing Normal University, Nanjing, China.

^jAlso at The University of Iowa, Iowa City, Iowa, USA.

- ^kAlso at University of Chinese Academy of Sciences, Beijing, China.
- ^lAlso at China Center of Advanced Science and Technology, Beijing, China.
- ^mAlso at University of Chinese Academy of Sciences, Beijing, China.
- ⁿAlso at China Spallation Neutron Source, Guangdong, China.
- ^oAlso at Henan Normal University, Xinxiang, China.
- ^pAlso at Université Libre de Bruxelles, Bruxelles, Belgium.
- ^qAlso at University of Latvia (LU), Riga, Latvia.
- ^rAlso at Another institute or international laboratory covered by a cooperation agreement with CERN.
- ^sAlso at Suez University, Suez, Egypt.
- ^tAlso at British University in Egypt, Cairo, Egypt.
- ^uAlso at Purdue University, West Lafayette, Indiana, USA.
- ^vAlso at Université de Haute Alsace, Mulhouse, France.
- ^wAlso at Istinye University, Istanbul, Turkey.
- ^xAlso at Tbilisi State University, Tbilisi, Georgia.
- ^yAlso at The University of the State of Amazonas, Manaus, Brazil.
- ^zAlso at Erzincan Binali Yildirim University, Erzincan, Turkey.
- ^{aa}Also at University of Hamburg, Hamburg, Germany.
- ^{bb}Also at RWTH Aachen University, III. Physikalisches Institut A, Aachen, Germany.
- ^{cc}Also at Isfahan University of Technology, Isfahan, Iran.
- ^{dd}Also at Bergische University Wuppertal (BUW), Wuppertal, Germany.
- ^{ee}Also at Brandenburg University of Technology, Cottbus, Germany.
- ^{ff}Also at Forschungszentrum Jülich, Juelich, Germany.
- ^{gg}Also at CERN, European Organization for Nuclear Research, Geneva, Switzerland.
- ^{hh}Also at Institute of Physics, University of Debrecen, Debrecen, Hungary.
- ⁱⁱAlso at Institute of Nuclear Research ATOMKI, Debrecen, Hungary.
- ^{jj}Also at Universitatea Babeş-Bolyai—Facultatea de Fizica, Cluj-Napoca, Romania.
- ^{kk}Also at Physics Department, Faculty of Science, Assiut University, Assiut, Egypt.
- ^{ll}Also at HUN-REN Wigner Research Centre for Physics, Budapest, Hungary.
- ^{mm}Also at Punjab Agricultural University, Ludhiana, India.
- ⁿⁿAlso at University of Visva-Bharati, Santiniketan, India.
- ^{oo}Also at Indian Institute of Science (IISc), Bangalore, India.
- ^{pp}Also at Birla Institute of Technology, Mesra, Mesra, India.
- ^{qq}Also at IIT Bhubaneswar, Bhubaneswar, India.
- ^{rr}Also at Institute of Physics, Bhubaneswar, India.
- ^{ss}Also at University of Hyderabad, Hyderabad, India.
- ^{tt}Also at Deutsches Elektronen-Synchrotron, Hamburg, Germany.
- ^{uu}Also at Department of Physics, Isfahan University of Technology, Isfahan, Iran.
- ^{vv}Also at Sharif University of Technology, Tehran, Iran.
- ^{ww}Also at Department of Physics, University of Science and Technology of Mazandaran, Behshahr, Iran.
- ^{xx}Also at Helwan University, Cairo, Egypt.
- ^{yy}Also at Italian National Agency for New Technologies, Energy and Sustainable Economic Development, Bologna, Italy.
- ^{zz}Also at Centro Siciliano di Fisica Nucleare e di Struttura Della Materia, Catania, Italy.
- ^{aaa}Also at Università degli Studi Guglielmo Marconi, Roma, Italy.
- ^{bbb}Also at Scuola Superiore Meridionale, Università di Napoli 'Federico II', Napoli, Italy.
- ^{ccc}Also at Fermi National Accelerator Laboratory, Batavia, Illinois, USA.
- ^{ddd}Also at Ain Shams University, Cairo, Egypt.
- ^{eee}Also at Consiglio Nazionale delle Ricerche—Istituto Officina dei Materiali, Perugia, Italy.
- ^{fff}Also at Riga Technical University, Riga, Latvia.
- ^{ggg}Also at Department of Applied Physics, Faculty of Science and Technology, Universiti Kebangsaan Malaysia, Bangi, Malaysia.
- ^{hhh}Also at Consejo Nacional de Ciencia y Tecnología, Mexico City, Mexico.
- ⁱⁱⁱAlso at Trincomalee Campus, Eastern University, Sri Lanka, Nilaveli, Sri Lanka.
- ^{jjj}Also at Saegis Campus, Nugegoda, Sri Lanka.
- ^{kkk}Also at National and Kapodistrian University of Athens, Athens, Greece.
- ^{lll}Also at Ecole Polytechnique Fédérale Lausanne, Lausanne, Switzerland.
- ^{mmm}Also at Universität Zürich, Zurich, Switzerland.
- ⁿⁿⁿAlso at Stefan Meyer Institute for Subatomic Physics, Vienna, Austria.
- ^{ooo}Also at Laboratoire d'Annecy-le-Vieux de Physique des Particules, IN2P3-CNRS, Annecy-le-Vieux, France.
- ^{ppp}Also at Near East University, Research Center of Experimental Health Science, Mersin, Turkey.
- ^{qqq}Also at Konya Technical University, Konya, Turkey.
- ^{rrr}Also at Izmir Bakircay University, Izmir, Turkey.

- ^{sss} Also at Adiyaman University, Adiyaman, Turkey.
- ^{ttt} Also at Bozok Universitetesi Rektörlüğü, Yozgat, Turkey.
- ^{uuu} Also at Marmara University, Istanbul, Turkey.
- ^{vvv} Also at Milli Savunma University, Istanbul, Turkey.
- ^{www} Also at Kafkas University, Kars, Turkey.
- ^{xxx} Also at Istanbul Okan University, Istanbul, Turkey.
- ^{yyy} Also at Hacettepe University, Ankara, Turkey.
- ^{zzz} Also at Istanbul University—Cerrahpasa, Faculty of Engineering, Istanbul, Turkey.
- ^{aaa} Also at Yildiz Technical University, Istanbul, Turkey.
- ^{bbb} Also at Vrije Universiteit Brussel, Brussel, Belgium.
- ^{ccc} Also at School of Physics and Astronomy, University of Southampton, Southampton, United Kingdom.
- ^{ddd} Also at University of Bristol, Bristol, United Kingdom.
- ^{eee} Also at IPPP Durham University, Durham, United Kingdom.
- ^{fff} Also at Monash University, Faculty of Science, Clayton, Australia.
- ^{ggg} Also at Università di Torino, Torino, Italy.
- ^{hhh} Also at Bethel University, St. Paul, Minnesota, USA.
- ⁱⁱⁱ Also at Karamanoğlu Mehmetbey University, Karaman, Turkey.
- ^{jjj} Also at California Institute of Technology, Pasadena, California, USA.
- ^{kkk} Also at United States Naval Academy, Annapolis, Maryland, USA.
- ^{lll} Also at Bingol University, Bingol, Turkey.
- ^{mmm} Also at Georgian Technical University, Tbilisi, Georgia.
- ⁿⁿⁿ Also at Sinop University, Sinop, Turkey.
- ^{ooo} Also at Erciyes University, Kayseri, Turkey.
- ^{ppp} Also at Horia Hulubei National Institute of Physics and Nuclear Engineering (IFIN-HH), Bucharest, Romania.
- ^{qqq} Also at Texas A&M University at Qatar, Doha, Qatar.
- ^{rrr} Also at Kyungpook National University, Daegu, Korea.
- ^{sss} Also at Universiteit Antwerpen, Antwerpen, Belgium.
- ^{ttt} Also at Yerevan Physics Institute, Yerevan, Armenia.
- ^{uuu} Also at Northeastern University, Boston, Massachusetts, USA.
- ^{vvv} Also at Imperial College, London, United Kingdom.
- ^{www} Also at Institute of Nuclear Physics of the Uzbekistan Academy of Sciences, Tashkent, Uzbekistan.